13

Nanofabrication of Particle Assemblies and Colloidal Crystal Patterns

Yoshitake Masuda
National Institute of Advanced Industrial Science and Technology (AIST), Anagahora, Shimoshidami, Moriyama-ku, Nagoya, Japan

1. Introduction

Nano/micro periodic structures have attracted much attention as next-generation devices[1,2] such as photonic crystals[3-5] in which the refractive index changes periodically to show a photonic band gap. Various scientific and engineering applications, such as control of spontaneous emission, zero-threshold lasing, sharp bending of light, and so on, are expected to become possible by using the photonic band gap and the artificially introduced defect states and/or light-emitters. The structures were prepared by semiconductor nanofabrication techniques such as lithography and etching processes[6,7], advanced wafer-fusion technique[8], lithographic layer-by-layer approach[9], holographic lithography[10], advanced silicon microelectromechanical systems[11], glancing angle deposition[12] or auto cloning technique[13], and theoretical studies were performed to estimate the properties of the structures. These studies confirmed the high potential of nano/micro periodic structures as future devices.

However, a simple process which requires a short time for fabrication, low energy and less amount of material needs to be developed to enable mass production. Additionally, the processes of patterning the structures need to integrate various elements for application to commercial devices. The regularity and feature edge acuity of periodic structures should also be improved in order to enhance the performance.

Nano/micro periodic structures can be prepared with short fabrication time and low energy by self-assembly of mono-dispersed particles in which particles and air (wall and air for inverse opal) are arranged periodically[14,15]. Self-assembly and patterning of nano/micro particles have attracted much attention recently[1,2,16,17]. Micropatterns of close-packed particle assemblies with high arrangement accuracy have been realized by using templates such as micromolds[18], grooves[19], cylindrical holes[20] or trenches[20]. However, substrates having micromolds or grooves are necessary in these processes, and feature edge acuity and regularity need to be improved further in order to fabricate various complicated structures for photonic devices.

In this section, nano/micropatterns of colloidal crystals were fabricated self-assembly. They were realized with several patterning methods in static solution systems[21-23] or in drying processes[24,25] without using molds or grooves. Microstructures constructed from particles such as micropatterns of particle layers, narrow particle wires, arrays of particle wires and so on were prepared under moderate conditions using self-assembled monolayers (SAMs).

Additionally, 2D patterning of colloidal crystals were realized with two solution method. The method has the advantage of both the static solution system and drying process. It offers excellent self-assembling performance for the fabrication of nano/micro periodic structures to be applied to next-generation devices.

2. Patterning of colloidal crystals in liquids[21-23]

2.1 Patterning of colloidal crystals in liquids

Novel processes to realize low-dimensional arrangement of SiO_2 particles were proposed[21-23]. Particle wires and a pattern of the close-packed particle monolayer were fabricated in the solution at room temperature. SAMs (self-assembled monolayers) were formed on Si substrates and modified to be suitable for templates of precise arrangement. Particles were arranged precisely in the desired positions in the solution using well controlled electrostatic interactions and chemical bond formation between particles and substrates.

2.2 SAM Preparation for patterning of coloidal crystals

Octadecyltrichlorosilane (OTS)-SAM was prepared by immersing the Si substrate in an anhydrous toluene solution containing 1 vol% OTS for 5 min under a N_2 atmosphere. SAMs were exposed for 2 h to UV light (184.9 nm) through a photomask. The UV-irradiated regions became hydrophilic due to Si-OH group formation, while the non-irradiated part remained unchanged, i.e., it was composed of hydrophobic octadecyl groups, which gave rise to patterned OTS-SAM. To check successful film formation and functional group change, water drop contact angles were measured for irradiated and non-irradiated surfaces. Initially deposited OTS-SAM had a water contact angle of 96°, while the UV-irradiated SAM surface was saturated (contact angle < 5°).

The patterned OTS-SAM was immersed in a toluene solution containing 1 vol% APTS (aminopropyltriethoxysilane) in air for 1 h. APTS molecules combined to silanol groups of SAM and hence, octadecyl / amino groups pattered SAM was fabricated. OTS-SAM exhibited a water contact angle of 96°, while that of the amino surface was 28°. These observations indicated successful fabrication of octadecyl / amino-groups patterned SAM.

2.3 Surface modification of SiO_2 particles

Silica particles (1μmφ, HIPRESICA UF, UNK, Ltd.) were immersed in a dicyclohexyl and sonicated for 10 min under a N_2 atmosphere for good dispersion. 1 vol% of trichlorocyanoethylsilane (TCES) was added to the dicyclohexyl solution under a N_2 atmosphere, and the solution was stirred gently for 30 min in order to chemisorb TCES onto the SiO_2 particle surfaces. SiO_2 particles with TCES were centrifuged several times to remove unreacted TCES using dicyclohexyl.

The SiO_2 particles with TCES were further dispersed in a tetrahydrofuran solution containing potassium tert-butoxide (t-BuOK) and 18-crown 6-ether for 48 h under an ambient atmosphere to oxidize the CN-groups to carboxyl groups. The solution was centrifuged several times using distilled water to remove t-BuOK, 18-crown 6-ether, and a tetrahydrofuran. SiO_2 particles modified with carboxyl groups were thus obtained.

SiO_2 particles covered by silanol groups or carboxyl groups were arranged selectively in silanol regions or amino regions of SAM using interactions between particles and SAMs. Zeta potentials of SiO_2 particles that have silanol groups and SiO_2 particles modified by carboxyl groups were measured (Zetasizer 3000HSA, Malvern Instruments Ltd.) as shown

in Fig. 1. Zeta potentials measured in aqueous solutions (pH=7.0) for the surface of silicon substrate covered with silanol groups, phenyl groups (PTCS) and amino groups (APTS) are –38.23 mV, +0.63 mV and +22.0 mV, respectively.

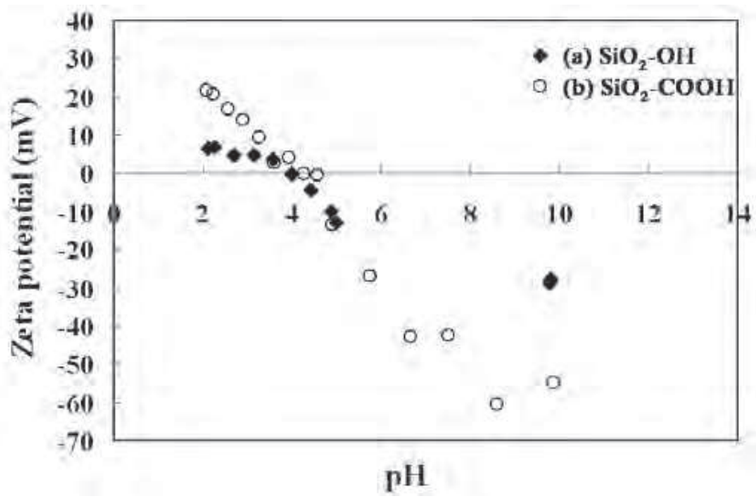

Reprinted with permission from Ref. [23], Masuda, Y., Itoh, M., Yonezawa, T. and Koumoto, K., 2002, *Langmuir*, 18, 4155. Copyright @ American Chemical Society

Fig. 1. Zeta potential of (a) SiO_2 particles and (b) SiO_2 particles modified with carboxyl groups.

2.4 Fabrication of particle wires employing selective arrangement process

OTS-SAM was modified by a diamond tip to form a line of silanol groups of approximately 0.5 μm width (Fig. 2). The diamond tip was contacted to OTS-SAM surface lightly and traced with low contact pressure in order to modify the SAM surface. The surface modified by a diamond tip, i.e., the white area in Figure 2 corresponds to silanol groups, showed low contact angle (<5°). This modified region was shown to be white compared with OTS-SAM region in a scanning electron micrograph (SEM; S-3000N, Hitachi, Ltd.). Octadecyl groups were broken mechanically by contact pressure with the diamond tip, and they possibly changed into silanol groups. The diamond tip was used to avoid contamination from a metal tip and the influence of a chemical reaction between the tip and the SAM.

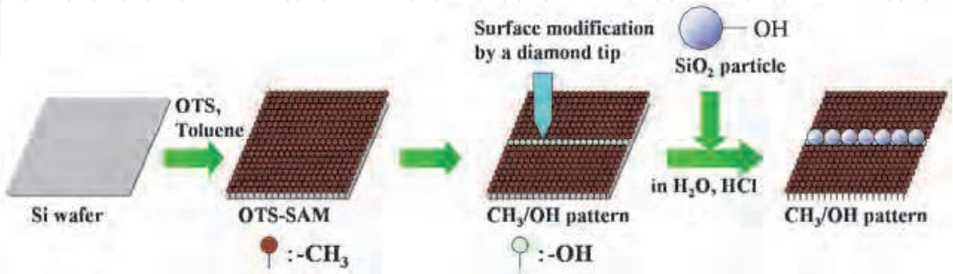

Reprinted with permission from Ref. [23], Masuda, Y., Itoh, M., Yonezawa, T. and Koumoto, K., 2002, *Langmuir*, 18, 4155. Copyright @ American Chemical Society

Fig. 2. Conceptual process for fabrication of a particle wire on a patterned SAM modified by a diamond tip.

Patterned SAMs were immersed in the aqueous solution containing SiO_2 particles and a hydrochloric acid as a condenser, rinsed in water, and were observed by a SEM. SiO_2 particles were observed on lines of silanol groups selectively indicating particles were successfully arranged well (Fig. 3(a)). Because particles were not easily removed by sonication, it was judged that iloxane bonds had been formed by condensation of silanol groups between particles and a SAM.

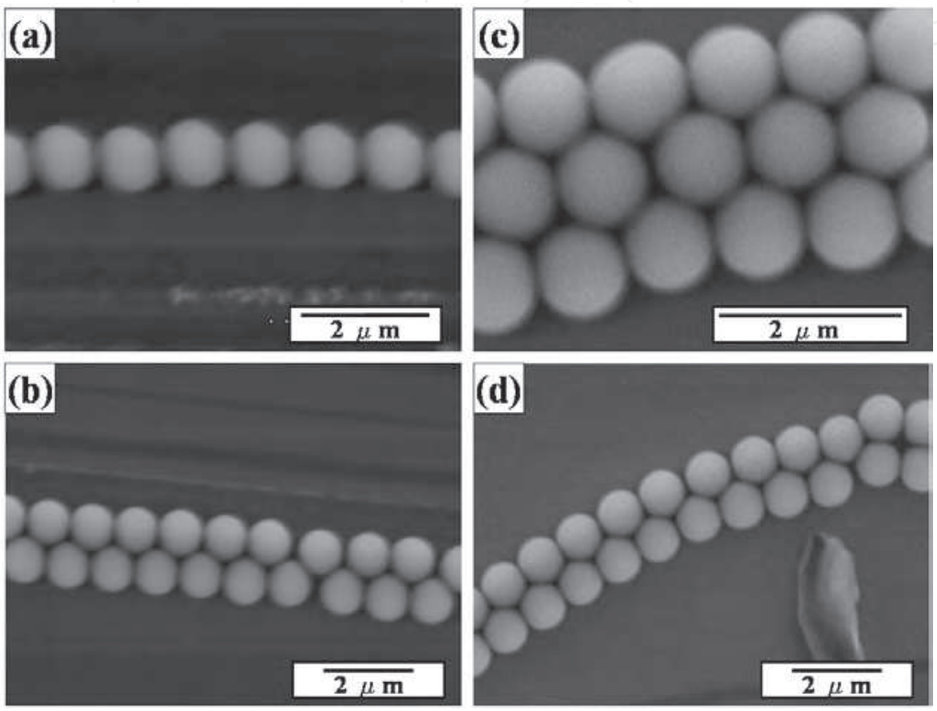

Reprinted with permission from Ref. [23], Masuda, Y., Itoh, M., Yonezawa, T. and Koumoto, K., 2002, *Langmuir*, 18, 4155. Copyright @ American Chemical Society

Fig. 3. SEM micrographs of (a) a single particle wire, (b) a double particle wire, (c) a triple particle wire and (d) a curved double particle wire

It is clearly seen that the accuracy of particle arrangement has been improved compared to our former experiments[21,22]. A double particle wire and a triple particle wire were likewise fabricated on wide silanol groups regions with about 1.4 μm and 2.2 μm in width, respectively (Fig. 3(b), (c)). The double particle wire that has a triangular lattice also demonstrates a high arrangement accuracy, though there is a defect in arrangement between seventh particle from left and eighth particle. Additionally, a curved double particle wire was fabricated on curved region of silanol groups. Curved double particle wires have not been reported previously, and they may have useful applications for an optical waveguide.
Accuracy of particle arrangement was evaluated from Fig. 3(a). Center position ((x_i, y_i) μm) of each particle was plotted to estimate the standard deviation (Fig. 4). The bottom left corner of Fig. 3(a) was set to be the origin of the x-y coordinate. The approximated straight line($f(x)$) and its slope (θ) are represented as follows.

$$f(x) = 0.0061x + 2.9609 \tag{1}$$

$$\cos\theta = 0.9940 \tag{2}$$

Standard deviation from the approximated straight line is described by the expression,

$$\text{S (standard deviation)} = \frac{\left[\sum_i \{\cos\theta \cdot (f(x_i) - y_i)\}^2\right]^{1/2}}{n-1} \tag{3}$$

where n is the number of particles (n = 6). S = 0.0126 was obtained. The accuracy of particle arrangement in Fig. 3(b) and (c) was estimated by the same manner. Standard deviation of seven particles from left in an upper particle line and an bottom particle line in Fig. 3(b) were estimated to be S = 5.66x10^{-3} and S = 3.84x10^{-3}. And standard deviation of an upper particle line, a middle particle line and a bottom particle line in Fig. 3(c) were estimated to be S = 8.11x10^{-4}, 8.27x10^{-3} and 2.30x10^{-2}, respectively.

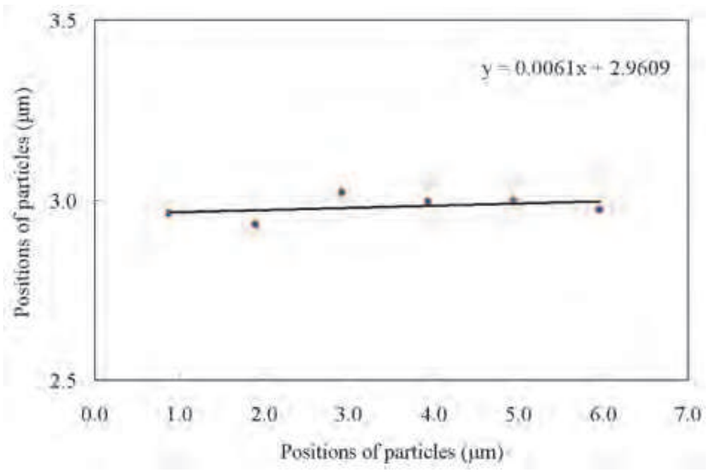

Reprinted with permission from Ref. [23], Masuda, Y., Itoh, M., Yonezawa, T. and Koumoto, K., 2002, *Langmuir*, 18, 4155. Copyright @ American Chemical Society

Fig. 4. Positions of particles in Fig. 3 (a) showing the accuracy of particle arrangement.

2.5 Precise arrangement of particles on small-area silanol sites modified by AFM lithograph

OTS-SAM was modified to silanol groups by an AFM (atomic force microscope, Nanoscope E, Digital Instruments) to control position of arrangement accurately (Fig. 5). A source measure unit (SMU Model 236, Keithley) was installed in the AFM in order to control the electric current passing through the probe and a SAM. The SAM was biased positively, and the AFM probe was scanned with constant current mode (50 nA), and the scanned area was used as a template for arrangement. Scanning area (100 nm×100 nm) was set smaller than the diameter of the particles (500 nmφ) to facilitate precise arrangement ofparticles.

SiO_2 particles (500 nmφ, powder, Admatechs Co., Ltd., SO-E2) modified with carboxyl groups were sonicated for 10 min in tetrahydrofuran or dichloromethane, and this solution was refrigerated to -20 ℃ for 1 h. N,N′-dicyclohexylcarbodiimide was added to this solution as a condenser to form ester bonds between carboxyl groups of SiO_2 particles and silanol

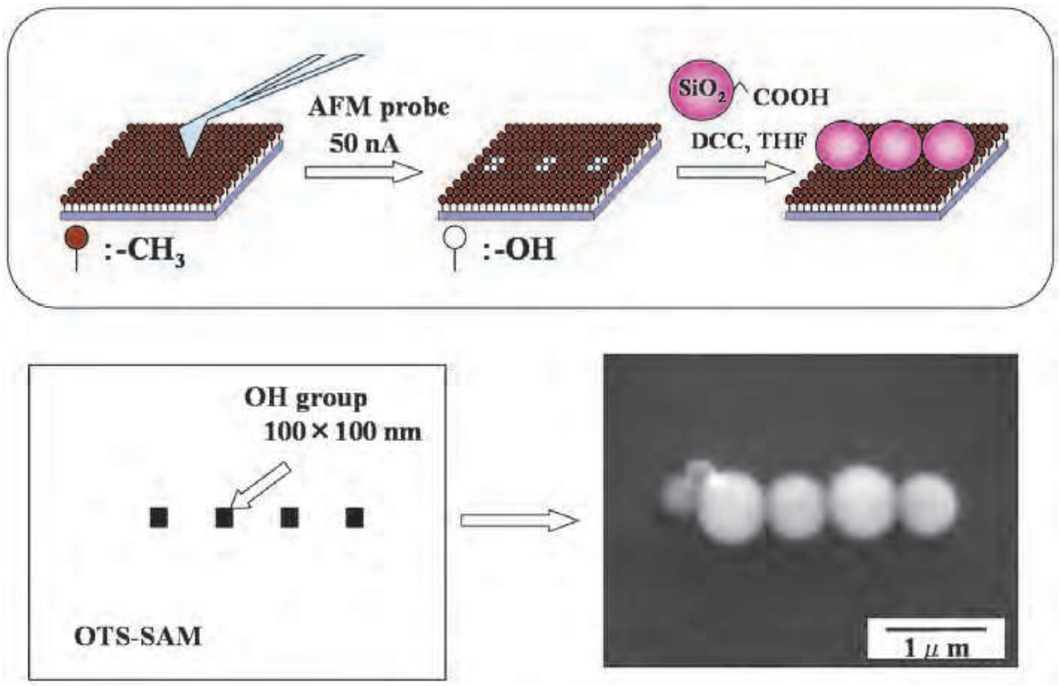

Reprinted with permission from Ref. [23], Masuda, Y., Itoh, M., Yonezawa, T. and Koumoto, K., 2002, *Langmuir*, 18, 4155. Copyright @ American Chemical Society

Fig. 5. Conceptual process and SEM micrograph of particle arrangement on a patterned SAM modified by AFM lithography.

groups of a SAM. Modified OTS-SAM was then immersed in this solution for 2 h. The temperature of the solution was increased slowly to 25 ℃ and kept for 2 h. After having been rinsed in water, a SAM was observed by a SEM. Particles were arranged in silanol regions and line of particle was fabricated (Fig. 5). Two-dimensional arrangement with required features can easily be realized with this technique, though it takes a long time to modify a SAM with an AFM probe. Particles weren't removed easily from a SAM by sonication, indicating that ester bonds were formed by condensation. The accuracy of particle arrangement in Fig. 5 was estimated to be $S = 1.17 \times 10^{-2}$. This might be decreased by decreasing the dimension of each silanol region.

In order to verify the formation of ester bonds between carboxyl groups and silanol groups, bromopropionic acid, whose molecule has a carboxyl group at one end and a bromo group at the other, was reacted with silanol groups of a Si substrate using the same reaction scheme as used to attach SiO_2 particles to silanol groups. After having been sonicated in acetone for 5 min, the substrate surface was analyzed by X-ray photoelectron spectroscopy (XPS; ESCALAB 210, VG Scientific Ltd., $1\text{-}3 \times 10^{-7}$ Pa, measurement area; 3 mm×4 mm). The X-ray source (MgK*a*, 1253.6 eV) was operated at 15 kV and 18 mA. The spectrum corresponding to Br 3d binding energy centering at 74.35 eV was observed. Although the observed binding energy is higher than that of KBr, this chemical shift must have been caused by carbon atoms neighboring bromine atoms. Since bromo groups can't react directly with silanol groups under the present conditions, the XPS result firmly indicates that carboxyl groups of bromopropionic acid reacted with silanol groups to form possible ester bonds.

2.6 Patterning of close-packed particle monolayers

SiO_2 particles modified with carboxyl groups were dispersed in water. Octadecyl / amino-groups patterned SAM was then immersed in the solution for several minutes (Fig. 6). The substrate was rinsed with water and observed with a SEM. SiO_2 particles were observed in silanol regions selectively forming a close-packed mono-particle layer (Fig. 7 (a)). Boundaries between the mono-particle layer and otcadecyl region is clearly observable, and a few particles are observed in octadecyl region. SiO_2 particles modified with carboxyl groups are charged negative, and amino groups of SAM are charged positive in water. Accordingly, particles are attracted to amino groups and form a mono-particle layer. Particles in the solution did not adhere to the mono-particle layer, since both the particles and the mono-particle layer have negative charges and repel each other. Particles were also deposited randomly in some areas (Fig. 7 (b)), and this suggests that it is difficult to obtain the pattern of the close-packed particle monolayer in a large area.

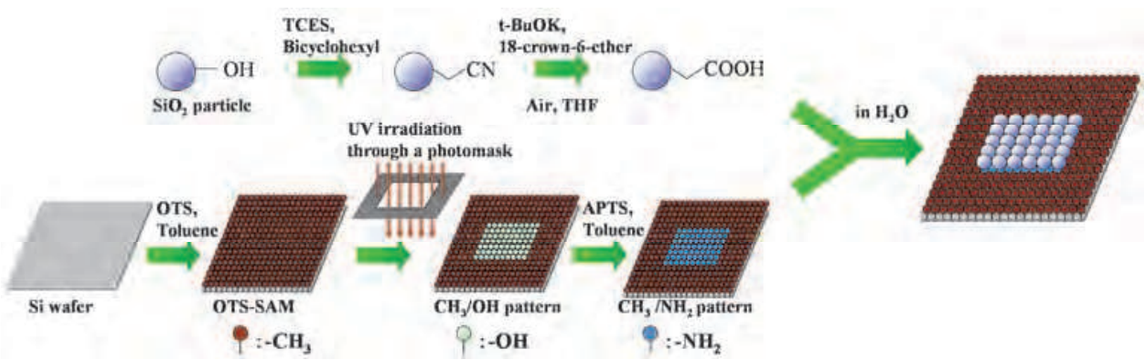

Reprinted with permission from Ref. [23], Masuda, Y., Itoh, M., Yonezawa, T. and Koumoto, K., 2002, *Langmuir*, 18, 4155. Copyright @ American Chemical Society

Fig. 6. Conceptual process for patterning of the close-packed particle monolayer.

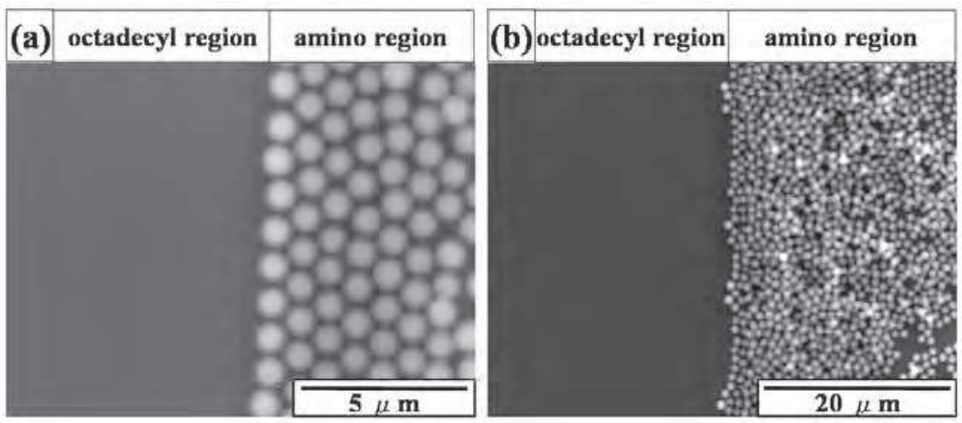

Reprinted with permission from Ref. [23], Masuda, Y., Itoh, M., Yonezawa, T. and Koumoto, K., 2002, *Langmuir*, 18, 4155. Copyright @ American Chemical Society

Fig. 7. SEM micrographs of (a) a close-packed particle monolayer of SiO_2 particles modified with carboxyl groups formed in the amino region and (b) randomly deposited particles in the amino region.

Additionally, octadecyl / amino-groups patterned SAM was immersed in the solution containing non-modified SiO_2 particles for several minutes (Fig. 8). While SiO_2 particles were observed in silanol region predominantly, the feature edge acuity of the pattern was lower than that of the pattern in which SiO_2 particles modified with carboxyl groups was used. This demonstrates applicability of surface modification of SiO_2 particles with carboxyl groups. Furthermore, octadecyl / silanol-groups patterned SAMs were immersed in solutions containing SiO_2 particles modified with carboxyl groups or non-modified SiO_2 particles for several minutes, respectively. Particles were not adhered to either octadecyl groups or silanol groups. This means that the difference in surface potential between SiO_2 particles modified with carboxyl groups and amino groups of SAM accelerate the adhesion of particles to the amino groups. Particles were attracted and adhered to amino groups predominantly by electrostatic interactions between particles and SAMs and chemical bonds weren't formed because pure water was used as a solution with no condensation agent. Surface of SiO_2 particles modified with carboxyl groups and amino SAM must have changed into $–COO^-$ and $–NH_3^+$, respectively, in water to attract each other.

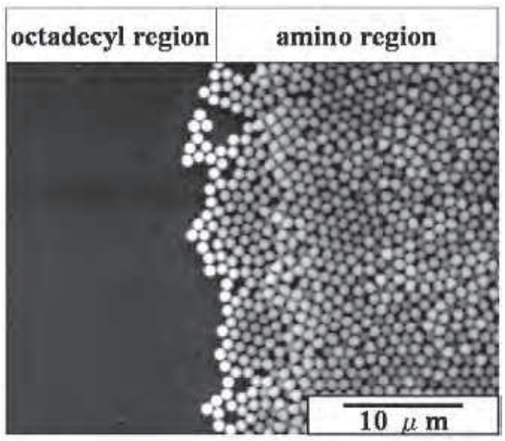

Reprinted with permission from Ref. [23], Masuda, Y., Itoh, M., Yonezawa, T. and Koumoto, K., 2002, *Langmuir*, 18, 4155. Copyright @ American Chemical Society

Fig. 8. SEM micrograph of randomly deposited SiO_2 particles in the amino region.

3. Drying patterning of colloidal crystals and 2D arrays

3.1 Self-assembly patterning of colloidal crystals by drying patterning[24]

Particle wires were fabricated through self-assembly on hydrophilic regions of SAMs (self-assembled monolayer)[24]. An SAM of octadecyltrichlorosilane was formed on a silicon substrate and modified by UV irradiation to create a pattern of hydrophobic octadecyl and hydrophilic silanol groups. Ethanol or water containing particles (550 nmφ or 800 nmφ) was dropped onto a patterned SAM. The solution was separated into two droplets with a liquid bridge between the droplets along the hydrophilic regions of a patterned SAM. The droplets and the liquid bridge were used as a mold for fabrication of a two-dimensional pattern of colloid crystals. Particle wire was formed between two droplets and colloid crystals such as an opal structure were formed at both ends of the particle wire after drying the solution. The particle wires constructed from a close-packed structure or non-close-packed structure, i.e. square lattice, were fabricated through self-assembly at room temperature using this method.

The UV-irradiated regions became hydrophilic due to the formation of Si-OH groups, while the non-irradiated part remained unchanged, i.e. it was composed of hydrophobic octadecyl groups, which gave rise to patterned OTS-SAM. To confirm successful film formation and functional group change, water drop contact angles were measured for irradiated and non-irradiated surfaces. Initially deposited OTS-SAM had a water contact angle of 96°, while the UV-irradiated SAM surface was saturated (contact angle $<5°$). This observation indicated successful fabrication of SAM patterned with octadecyl/silanol groups (Fig. 9). Polystyrene particles in water (150 μl) (550 nmϕ particle or 820 nmϕ carboxylated particle, 10% wt, dispersed in water, Seradyn Co., Ltd.) were further dispersed in ethanol (3 ml) or water (3 ml), and poured onto a patterned OTS-SAM. The contact angles of the ethanol solution or water solution measured 10-20° or 96° on the OTS-SAM, respectively, while they were saturated (contact angle <5°) on silanol groups. The droplets were observed to separate into two drops and a bridge of solution was formed on a silanol line. The droplets and the liquid bridge were used as a mold for fabrication of a two-dimensional pattern of colloid crystals. After evaporation of the solution, substrates were observed by a scanning electron microscope (SEM; S-3000N, Hitachi, Ltd.).

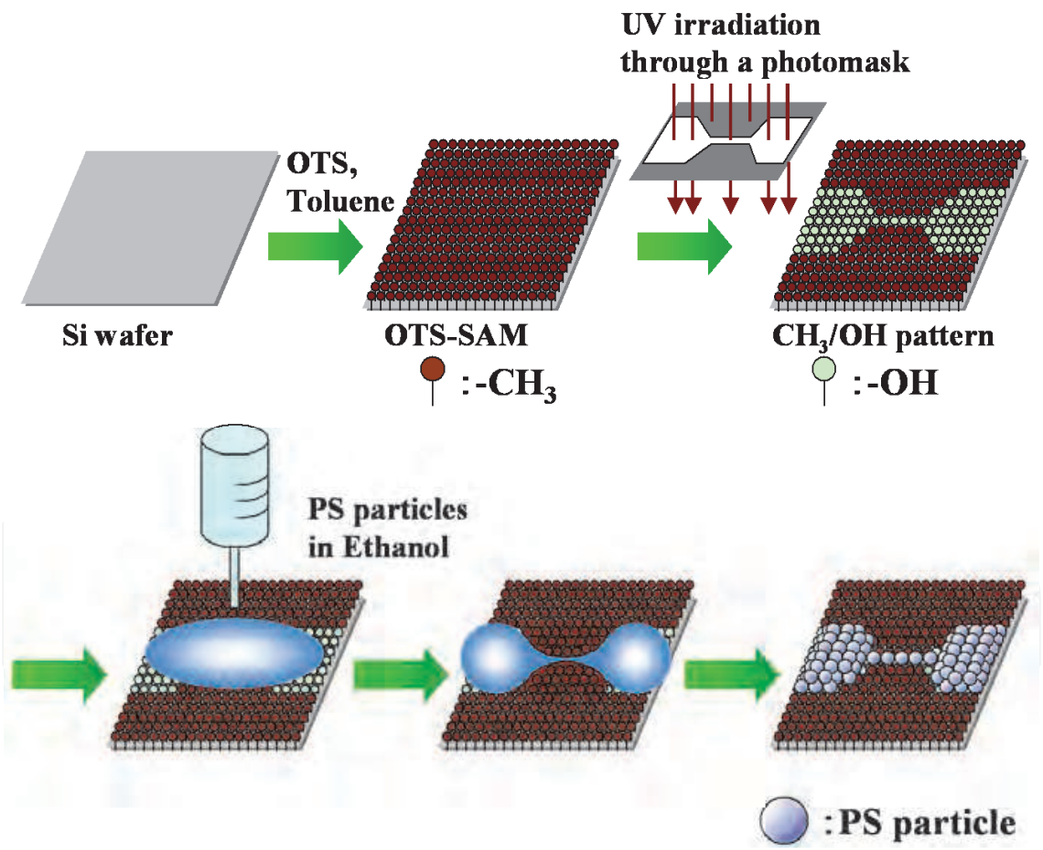

Reprinted with permission from Ref. [24], Masuda, Y., Tomimoto, K. and Koumoto, K., 2003, *Langmuir*, 19, 5179. Copyright @ American Chemical Society

Fig. 9. Conceptual process for fabrication of a particle wire using a patterned SAM and a liquid bridge.

The dispersibility of particles in the solution is very important for particle assembly and high dispersibility is necessary to form a close-packed structure. The zeta potentials of particles dispersed in the solutions were examined by direct measurement of electrophoretic mobility using an electrophoretic light scattering spectrometer (Zetasizer 3000HS, Malvern Instruments Co., Ltd.). The zeta potentials of polystyrene particles (550 nmϕ) in water, carboxylated particles (820 nmϕ) in water, polystyrene particles in ethanol and carboxylated particles in ethanol were determined to be -38.3 mV, -50.2 mV, -53.9 mV and -44.0 mV, respectively. Surface modification by carboxyl groups decreased the negative zeta potential in both solutions. Furthermore, particles in the ethanol had slightly low negative zeta potentials compared to those in water, i.e. the particles were slightly well-dispersed compared to those in water.

Polystyrene particles in water were poured onto a patterned OTS-SAM (Fig. 9), and observed after evaporation of the water. The water at the liquid bridge evaporated in about 24 h to form a particle wire, and droplets at the two ends completely evaporated in about 48 h. In this manner, particle wires constructed from a close-packed structure, i.e. triangular lattice, were produced from the water solution (Fig. 10a). The middle of a particle wire was narrower than its end (Fig. 10b, c). The width of the particle wire does not depend on the width of the silanol line, but rather on the interfacial tensions between solution and substrate, solution and atmosphere, and atmosphere and substrate. The silanol line was not used to decide the width of the particle wire, but rather the position of the liquid bridge and particle wire. Close-packed structures were also formed on large silanol regions (Fig. 10d, e). The right-hand area of Fig. 10d can be regarded as the {100} plane of the fcc structure and the left-hand area can be regarded as the {111} plane of the fcc structure or the {0001} plane of the hcp structure. The close-packed structure was thus considered to be an fcc structure.

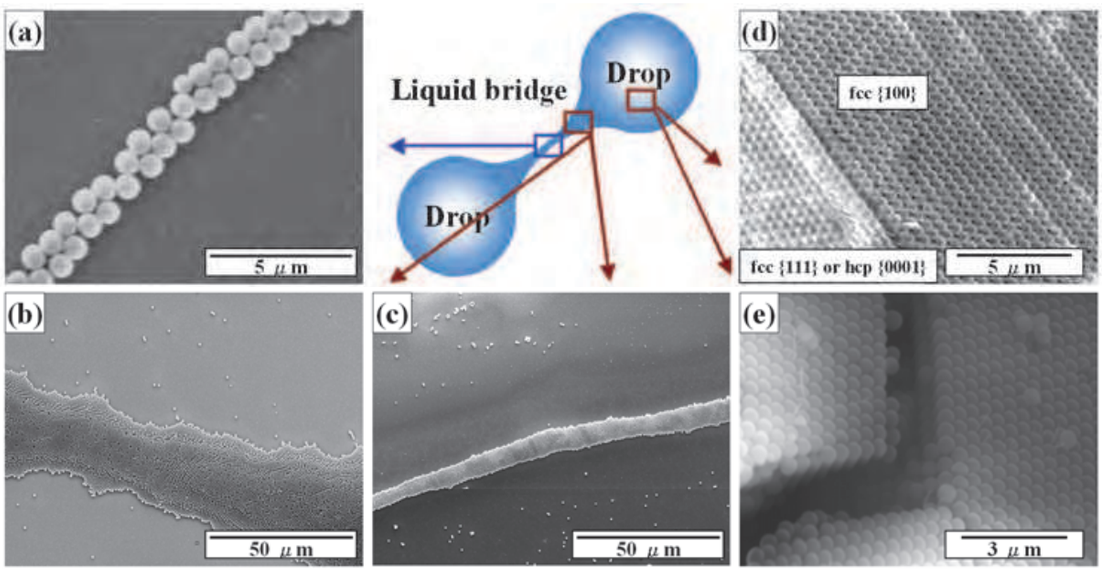

Reprinted with permission from Ref. [24], Masuda, Y., Tomimoto, K. and Koumoto, K., 2003, *Langmuir*, 19, 5179. Copyright @ American Chemical Society

Fig. 10. SEM micrographs of particle structures fabricated from aqueous solution containing micro particles using a liquid bridge. (a) - (c) particle wires constructed from triangular lattice (close-packed structure) and (d) - (e) a close-packed 3D structure.

Figure 11 shows particle wires and 3D structures fabricated from ethanol solution containing polystyrene particles. The ethanol at the liquid bridge evaporated in about 1 min to form a particle wire, and droplets at the two ends evaporated in about 20 min. The liquid bridge of ethanol evaporated faster than that of water for several reasons. The saturated vapor pressure of ethanol (59 mmHg (0.078 atm) at 25℃) is higher than that of water (24 mmHg (0.031 atm) at 25℃), explaining the difference in the evaporation rate of the two droplets. The ratio in evaporation rate of the ethanol liquid bridge to the ethanol droplets is higher than that of the water liquid bridge to the water droplets. This can be explained as follows: Water has high surface tension (71.8×10^{-3} N/m at 25℃) compared with ethanol (22.0×10^{-3} N/m at 25℃). Ethanol existed along patterned hydrophilic regions with small meniscus at the angle between droplets and a liquid bridge. However, water formed large meniscus at the angle between droplets and a liquid bridge, causing a wide line width of water liquid bridge compared with ethanol on our patterned surfaces. Additionally, the water liquid bridge was higher than that of ethanol due to high surface tension. These made the cross-section area of water larger than that of ethanol. The thick liquid bridge evaporated slowly because of its large volume and low vapor pressure calculated from the Kelvin equation in which the smaller convex liquid surface gives rise to higher internal pressure and faster evaporation rate. Furthermore, the solution at the droplets flowed into a liquid bridge and this further complicated the evaporation mechanism.

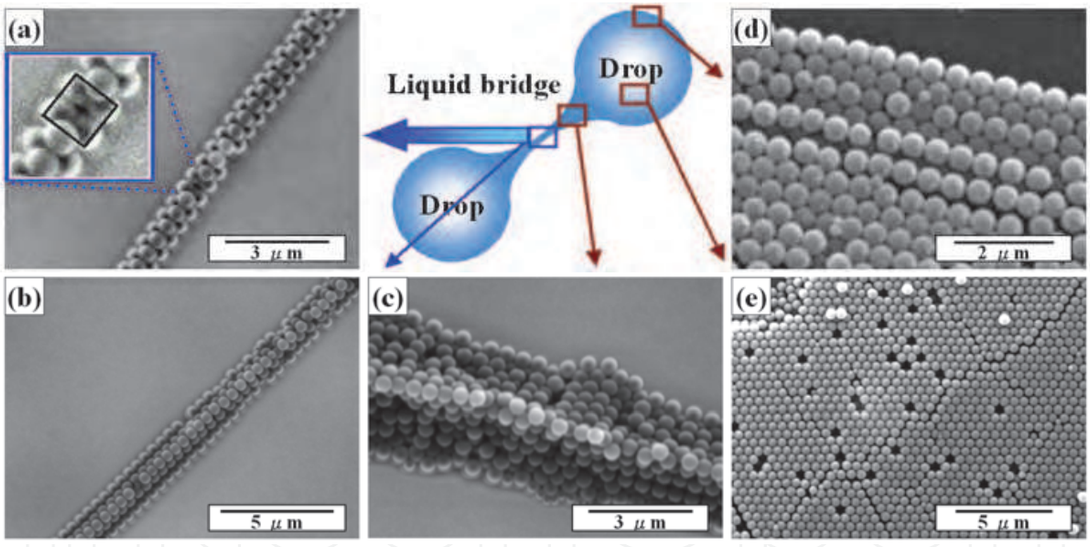

Reprinted with permission from Ref. [24], Masuda, Y., Tomimoto, K. and Koumoto, K., 2003, *Langmuir*, 19, 5179. Copyright @ American Chemical Society

Fig. 11. SEM micrographs of particle structures fabricated from ethanol solution containing micro particles using a liquid bridge. (a), (b) particle wires constructed from square lattice, (c) particles deposited on edge of silanol line and (d), (e) close-packed 3D structures.

A narrow particle wire was formed at the center of the liquid bridge (Fig. 11a, b), and wide wires were formed at the edges of the liquid bridge (Fig.11c) along the silanol line. The particle wire in Fig. 11a is not a close-packed structure and is constructed from a square lattice, which is a metastable phase compared with a close-packed structure. High dispersibility of particles is necessary to form a close-packed structure in the solution.

However, the particles dispersed well in ethanol and the dispersibility of particles in ethanol is similar to that in water. This shows that the non-close-packed structure was caused not only by the influence of dispersibility but also by many other factors. Movement and rearrangement of deposited particles is necessary to construct a close-packed structure. However, the ethanol evaporated quickly and suppressed the movement of particles by liquid bridge force. Additionally, adhesion between particles and a substrate, and cohesion between particles probably caused moderate suppression of the rearrangement of particles. Factors such as evaporation rate, interaction force between particles, and interaction force between particles and a substrate were important in the packing process. Close-packed 3D structures were also formed on large silanol regions (Fig. 11d, e), and they contained many defects (Fig. 11e). The ethanol evaporated so quickly that the particles did not rearrange well to form a close-packed structure during evaporation of ethanol. This is one of the factors of forming a loosely packed structure. To directly evaluate the effect of the evaporation rate, a similar experiment using ethanol was conducted in a small airtight container with small pinholes to allow the ethanol to evaporate slowly. The size and number of pin holes were adjusted for ethanol at the liquid bridge to evaporate in about 24 h. The particle wire constructed from a close-packed structure was formed after about 24 h, and droplets at both ends were dried after about 48 h. The close-packed 3D structures were formed in large silanol regions. The number of defects was smaller than that formed from the ethanol solution with a shorter time and was similar to that formed from water. The humidity in the container was close to 100% and the saturated vapor pressure of ethanol was 59 mmHg (0.078 atm) at 25℃. This showed that particles dispersed well in ethanol and the interaction between particles and a substrate was sufficiently weak to produce a close-packed structure in the drying process of 24 h. Additionally, the results showed that not only the interaction force between particles and that between particles and a substrate, but also the evaporation rate needs to be controlled to fabricate particle wires.

Accuracy of particle arrangement was evaluated from Fig. 11(a) as calculated in recent work[23]. The center position ((x_i, y_i) μm) of each particle in an upper layer was plotted to estimate the standard deviation. The bottom left corner of Fig. 11(a) was set to be the origin of the x-y coordinate.

The approximated straight line ($f(x)$) and its slope (θ) are represented as follows.

$$f(x) = 1.3965x - 5.3344 \tag{4}$$

$$\cos\theta = 0.5822 \tag{5}$$

Standard deviation from the approximated straight line is described by the expression,

$$\text{S (standard deviation)} = \frac{\left[\sum_i \left\{\cos\theta \cdot \left(f(x_i) - y_i\right)\right\}^2\right]^{1/2}}{n-1} \tag{6}$$

where n is the number of particles (n = 19). The accuracy of the particle arrangement in Fig. 11(a) was estimated to be S = 1.63×10^{-3}. This is lower than that of the particle arrangement obtained in our previous work[23].

Particle wires were fabricated on hydrophilic regions of a patterned SAM. Ethanol or water containing particles was separated into two droplets with a liquid bridge between the droplets along hydrophilic regions of a patterned SAM. Particle wires constructed from a close-packed structure or non-close-packed structure were then formed through self-assembly between two droplets after drying of the solution.

3.2 Self-assembly 2DArray of colloidal crystal wires by drying patterning[25,26]

An orderly array of particle wires constructed from a close-packed colloidal crystal were fabricated without preparation of patterned templates[25,26]. A substrate was immersed vertically into a SiO_2 colloidal solution, and the liquid surface moved downward upon evaporation of solution. Particles formed a mono/multi-particle layer, which was cut by the periodic drop-off of solution. The orderly array of particle wires was successfully fabricated, showing the suitability of the self-assembly process for the fabrication of nano/micro structures constructed from nano/micro particles or blocks. The mechanism of the assembly process and control of thickness, width and interval of particle wires were further discussed. Moreover, an array of particle wires constructed not from close-packed fcc (or hcp) structure but from two kinds of particles was realized to fabricate an array of particle wires with NaCl structure by this self-assembly process.

Octadecyltrichlorosilane (OTS)-SAM was prepared by immersing Si substrate in an anhydrous toluene solution containing 1 %vol OTS for 5 min under an N_2 atmosphere. The contact angles of the ethanol solution or water solution measured 10-20° or 96° on the OTS-SAM, respectively. The water solution showed a contact angle of 10-20° on a silicon wafer that was kept in air.

The OTS-SAM was immersed in ethanol solution (80 ml) containing SiO_2 particles (1000 nmφ, 10 mg). The bottom of the solution was heated at 70°C and a condenser tube was kept at the top of the solution to cool it. The temperature difference between the top and bottom of the solution was controlled so as to stir and move particles by convection. The surface of the solution moved on the OTS-SAM surface upon evaporation of the ethanol. Particles began to assemble at the surface of the solution (Fig. 12(a)) and the particle layer was fabricated by movement of the solution surface (Fig. 12(b)). Further evaporation of the solution caused separation of the particle layer and solution surface (Fig. 12(c)) because particles were not sufficiently supplied from the solution. The liquid surface then dropped off and the particle layer separated from the solution surface (Fig. 12(d)). The next particle layer was formed by the same procedure (Fig. 12(e)). Consequently, separated particle wires, i.e. an array of particle wires, were successfully fabricated by our newly developed method (Fig. 12(f), 12(a-d)).

After having been immersed in the solution, which evaporates quickly, the substrates were observed using a scanning electron microscope (SEM; S-3000N, Hitachi, Ltd.), an optical microscope (BX51WI Microscope, Olympus Optical Co., Ltd.) with a digital camera (DP50, 5.8 megapixels, Olympus Optical Co., Ltd.) and a computer for capturing data, and a digital video camera recorder (DCR-TRV 50, Sony Corporation) with optical magnifying glass.

The width and interval of particle wires fabricated from the ethanol solution (80 ml) containing SiO_2 particles (10 mg) at 70°C were shown to be about 150 μm and 200 μm, respectively (Fig. 13(a-d)). Particle wires were constructed from a close-packed particle structure and their upper side showed high feature edge acuity (Fig. 13(c)). The array of

particles finished suddenly as shown on the bottom side of the particle wires (Fig. 13(c-d)). These observations suggest that particle wires were formed from the upper side and were cut by the drop-off of solution, and are consistent with the procedure shown in Fig. 12.

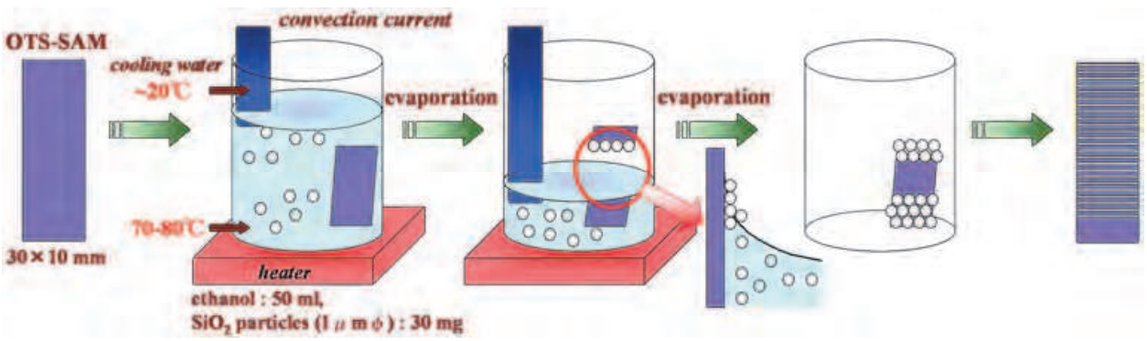

Reprinted with permission from Ref.[26], Masuda, Y., Itoh, T., Itoh, M. and Koumoto, K., 2004, *Langmuir*, 20, 5588. Copyright @ American Chemical Society

Fig. 12. Schematic for self-assembly process to fabricate an orderly array of particle wires constructed from a close-packed structure.

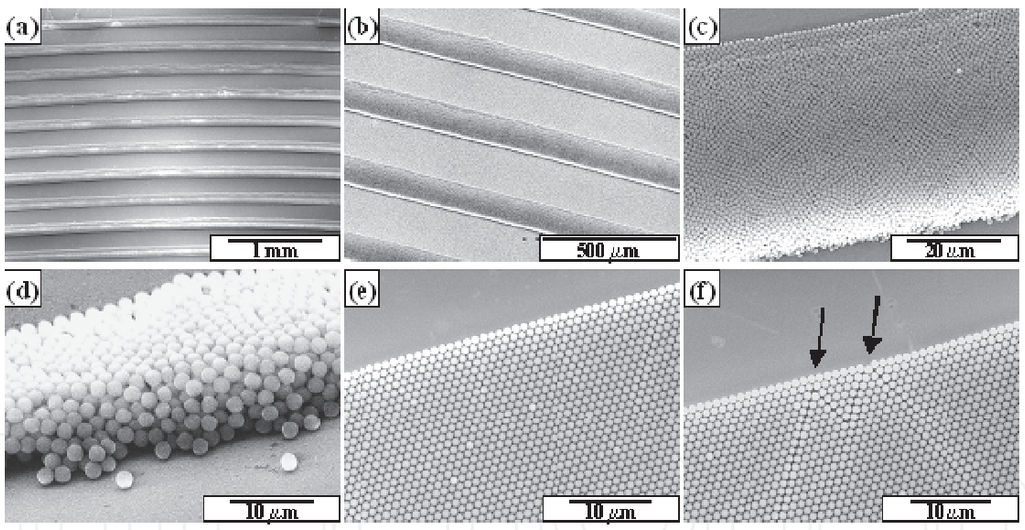

Reprinted with permission from Ref.[26], Masuda, Y., Itoh, T., Itoh, M. and Koumoto, K., 2004, *Langmuir*, 20, 5588. Copyright @ American Chemical Society

Fig. 13. SEM micrographs of array of particle wires constructed from (a-d) multiparticle layer or (e-f) monoparticle layer, (d) bottom side of a particle wire, (f) a monoparticle wire having two defects on the upper side.

Particle wires were formed on the OTS-SAM from the ethanol solution (80 ml) containing a small amount of SiO_2 particles (1000 nmφ, 1 mg) to fabricate thin wires constructed from a mono-particle layer (Fig. 13(e-f)). Particles were slowly supplied to particle wires from the solution. The number of particle layers was shown to be controlled by the change of particle number in the solution. The upper side of the particle wire in Fig. 13(f) has two defects, shown by arrows. The influence on the arrangement below the defects shows that particles

were constructed from the upper side to form a close-packed structure. In addition, the disorder disappeared at the middle of the particle wire (Fig. 13(f)), which shows that the formation process of particle wire has self-recovery ability.

Figure 14 shows the formation process of particle wire. The upper particle line was formed (Fig. 14(a)) first and particles were supplied gradually from the solution to form a close-packed structure (Fig. 14(b)) to prepare a wide mono-particle wire (Fig. 14(c)). High dispersibility of particles in the solution and the effective meniscus force allowed us to prepare a highly-ordered close-packed structure.

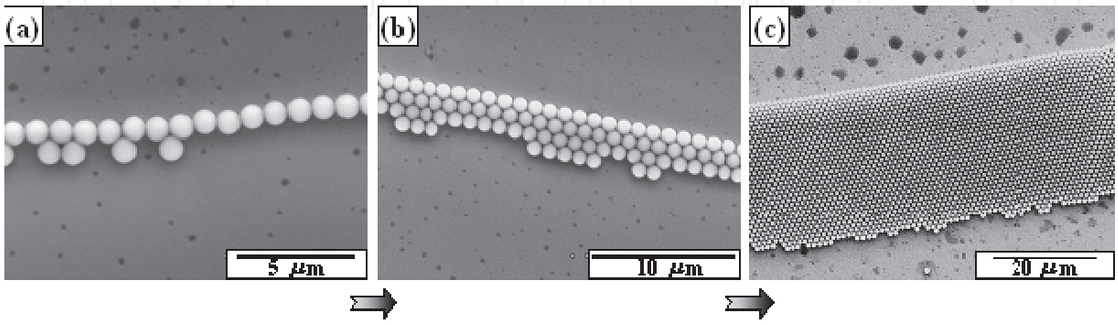

Reprinted with permission from Ref.[26], Masuda, Y., Itoh, T., Itoh, M. and Koumoto, K., 2004, *Langmuir*, 20, 5588. Copyright @ American Chemical Society

Fig. 14. SEM micrographs of the formation process of a particle wire.

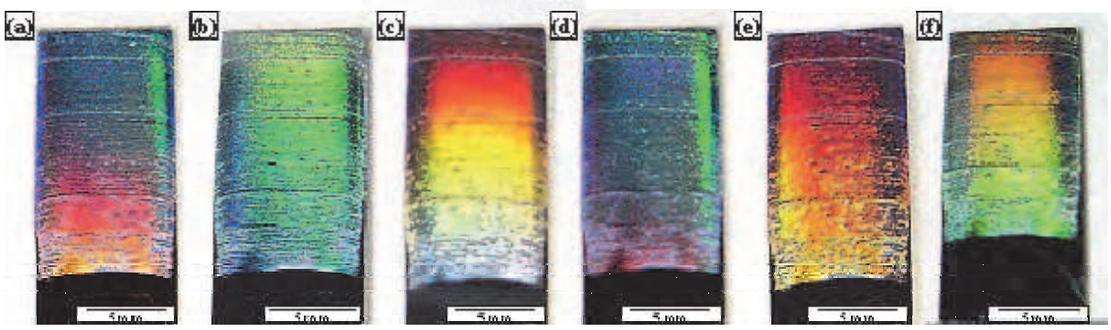

Reprinted with permission from Ref.[26], Masuda, Y., Itoh, T., Itoh, M. and Koumoto, K., 2004, *Langmuir*, 20, 5588. Copyright @ American Chemical Society

Fig. 15. Photographs of particle wires taken from different directions. (a) front view, (b-f) slightly cross shot of the same sample.

Particle wires showed iridescent diffraction (Fig. 15) caused by the high regularity of the particle array shown in Fig. 13. Diffracted wave number was changed drastically by the diffraction angle.

A close-packed structure was easily obtained by the use of meniscus force compared to the site-selective deposition in the solution[21-23]. A two-dimensional ordered array can be fabricated without the preparation of a template although templates are required for the liquid mold method[24].

Control of the interval of particle wires was achieved by change in solution temperature (Fig. 16, 17). The interval of particle wire fabricated from the ethanol solution (80 ml)

containing SiO_2 particles (20 mg) at 70°C (Fig. 16(a)) was about three times that of particle wires fabricated at 60°C (Fig. 16(b)) or 50°C (Fig. 16(c)) (Fig. 17). The same tendency was confirmed in the dilute solution system (80 ml) containing SiO_2 particles (10 mg) (Fig. 17). Wide interval was caused from high descent speed of solution surface at high temperature. The regularity of particle wires at 70°C was much higher than that at 60°C or 50°C in which the movement of particles caused by convection and the descent speed of solution surface was low compared to that at 70°C.

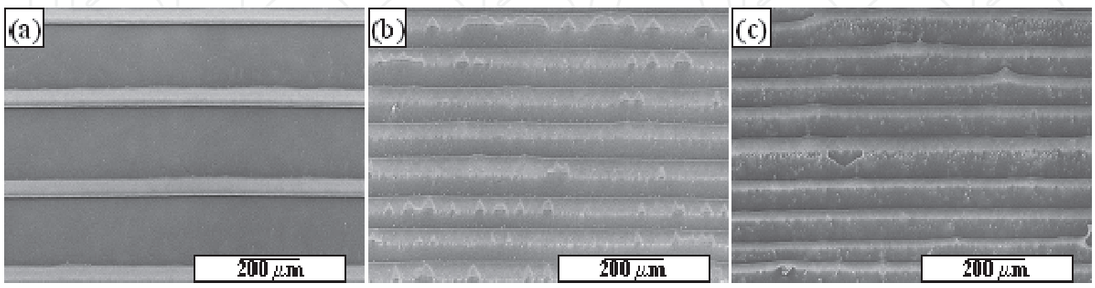

Reprinted with permission from Ref.[26], Masuda, Y., Itoh, T., Itoh, M. and Koumoto, K., 2004, *Langmuir*, 20, 5588. Copyright @ American Chemical Society

Fig. 16. SEM micrographs of array of particle wires constructed at (a) 70 °C, (b) 60 °C or (c) 50 °C.

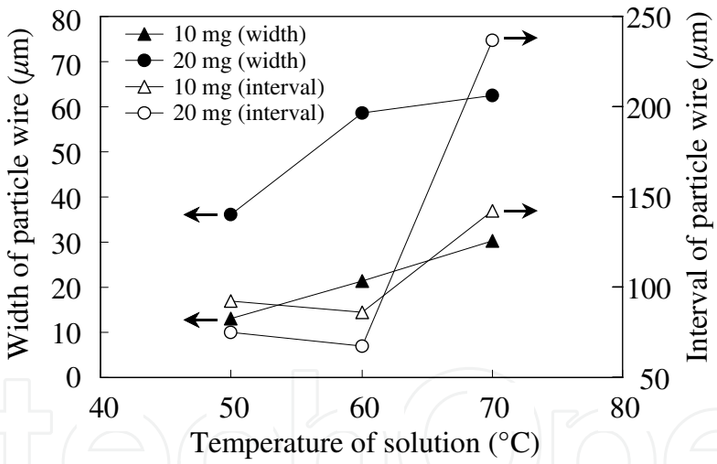

Reprinted with permission from Ref.[26], Masuda, Y., Itoh, T., Itoh, M. and Koumoto, K., 2004, *Langmuir*, 20, 5588. Copyright @ American Chemical Society

Fig. 17. Width and interval of particle wires as functions of temperature of solution.

The width of particle wires was also controlled by change in solution temperature or particle concentration in the solution (Fig. 17). The width of particle wires was increased by the increase of solution temperature in both particle concentrations (10 mg or 20 mg), and the width at high particle concentration (20 mg) was about two times that at low particle concentration (10 mg). High descent speed of solution surface and high movement of particles caused by convection were brought about at high temperature. These factors probably cause the change in width; however, further precise control and clarification of mechanism are necessary. Descent speed of solution surface would be controlled by control

of the lift speed of a substrate instead of control of the evaporation speed. Further improvement of the process is required for application to future devices.
Self-assembly of particle wires was realized using water instead of ethanol without an SAM (Fig. 18). The particle wires also showed iridescent diffraction and the diffracted wave number was changed drastically by the diffraction angle. A particle layer was reported to form on the whole area of OTS-SAM by the use of water, which evaporates slowly compared with ethanol. Fast movement of the solution surface caused by quick evaporation or lift of substrate is probably necessary for drop-off of the solution surface, which allows fabrication of separated particle wires. The condenser tube, which is used to cool the solution surface, was removed to evaporate water more quickly. This makes the descent speed of the water surface fast enough to separate the particle wires. Additionally, silicon wafer, which was kept in air to show a contact angle of 10-20° to water, was used instead of OTS-SAM. Because the contact angle of the water on the OTS-SAM (96°) was higher than that of ethanol (10-20°) the shape of the water surface was not suitable for making an array of particle wires. These improvements allowed us to fabricate an array of particle wires using water without an SAM. This process is environmentally friendly compared with the process using ethanol with OTS-SAM; however, the regularity and the feature edge acuity of particle wires were low compared to the process shown in Fig. 13 and thus further improvement is required in this system.

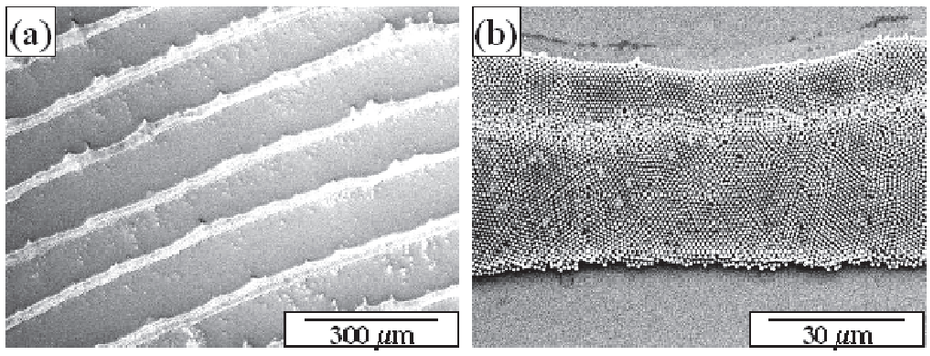

Reprinted with permission from Ref.[26], Masuda, Y., Itoh, T., Itoh, M. and Koumoto, K., 2004, *Langmuir*, 20, 5588. Copyright @ American Chemical Society

Fig. 18. SEM micrographs of array of particle wires fabricated from water solution.

Array of particle wires constructed not from fcc (or hcp), but from NaCl structure (rock salt structure) in which each ion is 6-coordinate and has a local octahedral geometry, was realized by the use of two kinds of particles (SiO_2 modified with carboxyl groups: 2000 nmφ, SiO_2 modified with amino groups: 1000 nmφ; ratio of particle radii is 0.5). SiO_2 particles 2000 nmφ in diameter and SiO_2 particles 1000 nmφ in diameter were modified to have carboxyl groups or amino groups on their surfaces, respectively. The zeta potential of SiO_2 particles modified with carboxyl groups was measured to be -40 mV in an aqueous solution at pH 7.0[8] by direct measurement of electrophoretic mobility using an electrophoretic light-scattering spectrometer (Zetasizer 3000HS, Malvern Instruments Co., Ltd.). On the other hand, APTS (3-Aminopropyltriethoxysilane)-SAM was prepared by the immersion of silicon wafer in an anhydrous toluene solution containing 1 vol% APTS for 1 h in air to measure the zeta potential instead of SiO_2 particles modified with amino groups. Amino groups of APTS-SAM were measured to be +22.0 mV in aqueous solutions (pH = 7.0) by an

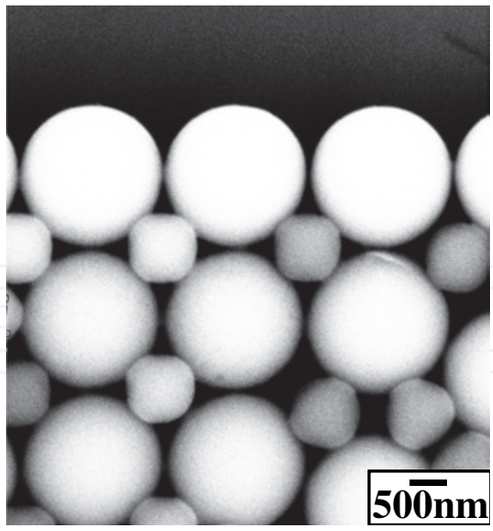

Reprinted with permission from Ref.[26], Masuda, Y., Itoh, T., Itoh, M. and Koumoto, K., 2004, *Langmuir*, 20, 5588. Copyright @ American Chemical Society

Fig. 19. SEM micrograph of array of particle wires constructed from NaCl structure.

electrophoretic light-scattering spectrophotometer (ELS-8000, Otsuka Electronics Co., Ltd.). Electrostatic interaction between SiO_2 particles modified with carboxyl groups and SiO_2 particles modified with amino groups was utilized for self-assembly of these particles to form ionic crystal such as NaCl structure. Although the ratio of ion radii is 0.611 (= $r^+(Na^+)/r^-(Cl^-)$) in NaCl, cations can contact to anions in the range of 0.414 – 0.732 in ratio of ion radii to form NaCl structure. Figure 19 shows the upper side of the particle wire and is the same arrangement as (100) face of NaCl structure. Each particle can be 6-coordinate when the same particle layer stacks on this layer with a slide of half lattice constant (sum of each particle radii). Small spherical particles (cations in NaCl structure) are shown as square or triangular in SEM micrographs because electrons from the SEM electron gun flowed from large particles into small particles to show the contacted area as white. Two kinds of dispersed particles would be adhered on the substrate and rearranged well to form 2-D layer. Particles were also deposited randomly in some areas, and this suggests that it is difficult to obtain NaCl structure in a large area. In addition, NaCl structure was prepared from two kinds of SiO_2 particles without surface modification (SiO_2: 2000 nmφ, SiO_2: 1000 nmφ; ratio of particle radii is 0.5) though the regularity of particle array was slightly lower than that prepared from SiO_2 particles with surface modification. NaCl-type arrangement of bimodal SiO_2 particles can be formed thermodynamically without electrostatic interaction because (100) face of NaCl structure constructed from large particles (x nmφ) and small particles $\left(\left(\sqrt{2}-1\right)\chi\text{nm}\varphi\right)$ was close-packed structure. This process should be improved to prepare NaCl structure without the use of surface modification of particles to apply for various kinds of particles. Additionally, the interaction between particles, substrates and liquid and the behavior of particles should be controlled well to form particle assembly having high regularity. Particles should be dispersed well in the solution to avoid aggregation, and attractive interaction between particles and a substrate should be decreased enough to accelerate rearrangement of particles on the substrate. Appropriate movement of particles accelerate formation of particles assembly, however, excess

convection suppresses assembly of particles. This process has many factors should be improved to fabricate particle assembly having desired structure and high regularity. The fabrication of an array of particle wire constructed from NaCl structure shows high ability of self-assembly process to realize future devices such as photonic crystal in which various structures are required to effectively utilize PBG.

Particle wires constructed from a close-packed multi-particle layer or mono-particle layer were fabricated without patterned templates. The array shows iridescent diffraction caused by high regularity of the particle array. The mechanism of the process was discussed and the control of the thickness, width and interval of particle wires was realized by change of solution temperature and concentration of colloidal solution. Furthermore, an array of particle wires constructed from an ionic crystal such as NaCl structure was fabricated using electrostatic interaction between particles showing positive zeta potential and particles showing negative zeta potential. This shows the suitability of the self-assembly process for creating future devices such as photonic crystals.

3. Patterning of colloidal crystals and spherical assemblies by two-solution method

3.1 Self-assembly patterning of colloidal crystals by two-solution method[27]

Desired patterns of colloidal crystals having high feature edge acuity and high regularity were fabricated by two-solution method[27]. A micropattern of colloidal methanol prepared on a self-assembled monolayer in hexane was used as a mold for particle patterning, and slow dissolution of methanol into hexane caused shrinkage of molds to form micropatterns of close-packed SiO_2 particle assemblies. This result is a step toward the realization of nano/micro periodic structures for next-generation photonic devices by a self-assembly process.

Silicon substrate was immersed into toluene solution containing 1 vol % octadecyltrichlorosilane (OTS) molecules under nitrogen atmosphere for 5 min to prepare a hydrophobic OTS-SAM. OTS-SAM was irradiated by ultraviolet light (PL21-200, SEN Lights Co., 18 mW/cm^2, distance from a lamp 30 mm, 24°C, humidity 73 %, air flow 0.52 m^3/min, 100 V, 320 W) through a photomask for 10 min. UV irradiation modified hydrophobic octadecyl groups to hydrophilic silanol groups forming a pattern of octadecyl regions and silanol regions. Patterned OTS-SAM having hydrophobic octadecyl regions and hydrophilic silanol regions was used as a template for patterning of colloidal solution.

SiO_2 particles (1 μm in diameter) (0.002 – 0.2 mg) were thoroughly dispersed in methanol (20 μl) and dropped on a patterned OTS-SAM (Fig. 20). The solution was lightly repelled by hydrophobic regions and mainly exists on hydrophilic silanol regions. The substrate was then immersed into hexane and carefully swung to remove the residual solution. The solution was repelled well by octadecyl regions in hexane. The contact angle of the methanol solution on OTS-SAM was confirmed to increase from 51.6° in air to 129.5° in hexane (Fig. 20), indicating that the methanol solution tends to exist on silanol regions selectively.

Methanol was then gradually dissolved into hexane to shrink the colloidal solution mold containing particles. The shrinkage of the mold increased the concentration of particles in the solution. The particles then attracted each other by meniscus force to form a close-packed fcc (face-centered cubic) or hcp (hexagonal closest packing) structure during the drying process of methanol. Close-packed structures were thus formed on hydrophilic silanol regions selectively (Fig. 21, A to H).

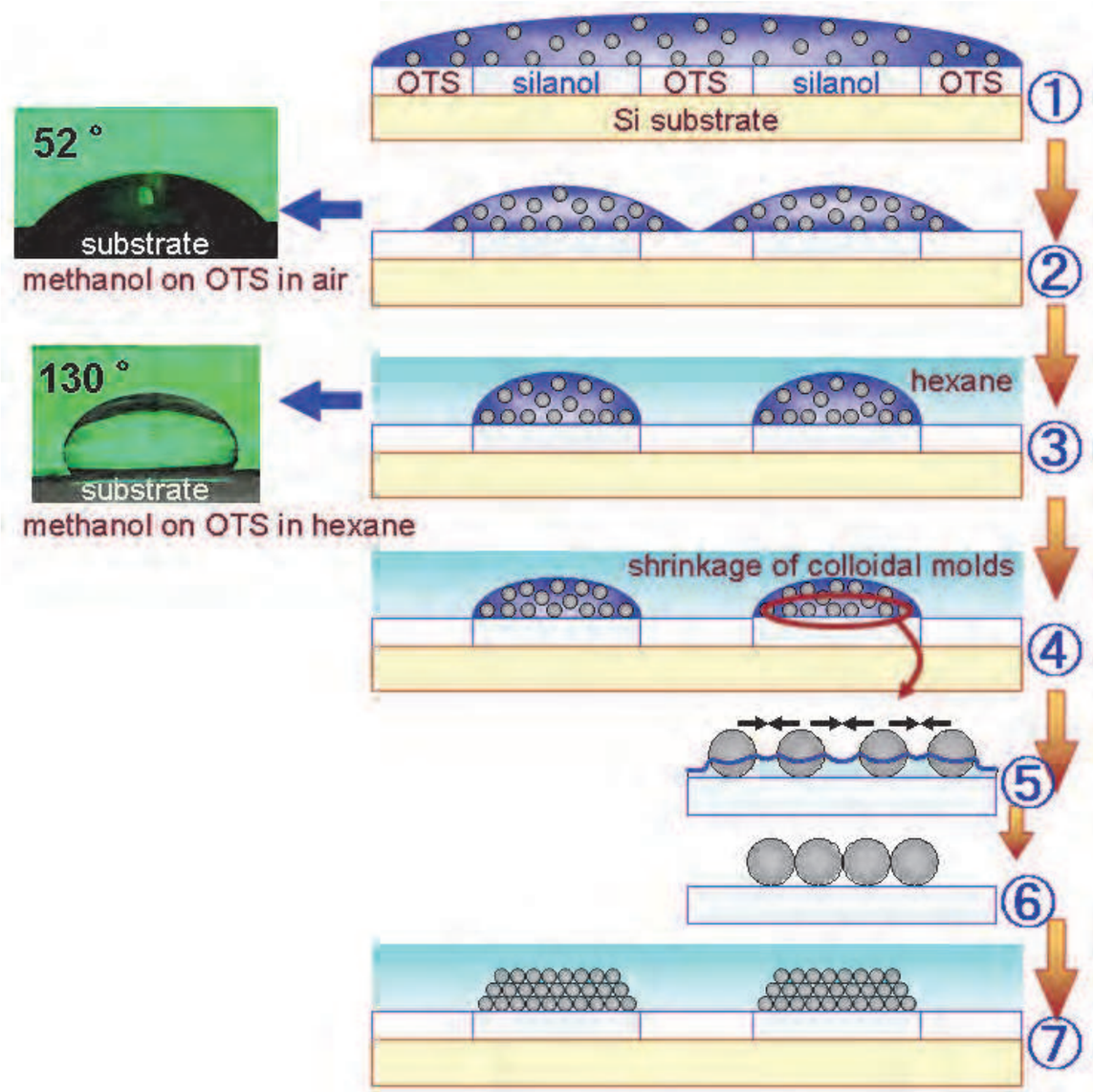

Reprinted with permission from Ref. [27], Masuda, Y., Itoh, T. and Koumoto, K., 2005, *Langmuir*, 21, 4478. Copyright @ American Chemical Society

Fig. 20. Conceptual process for two-solution self-assembly method to fabricate patterned colloidal photonic crystals.

2D micropatterns of multi particle-layers (Fig.21, A and B), partially double particle-layers (Fig. 21, C and D), or single particle-layers (Fig. 21, E to H) were successfully fabricated by changing the particle concentration in the solution and solution volume per unit of hydrophilic area (SiO_2/methanol0.2 mg/20 μl for Fig. 21, A and B, 0.02 mg/20 μl for Fig. 21, C and D, 0.002 mg/20 μl for Fig. 21, E to H). 2D patterns of colloidal crystals with high regularity in particle assembly have not been prepared by our processes previously reported[21-25]. The feature edge acuity of patterns and regularity in particle assembly[21-25]

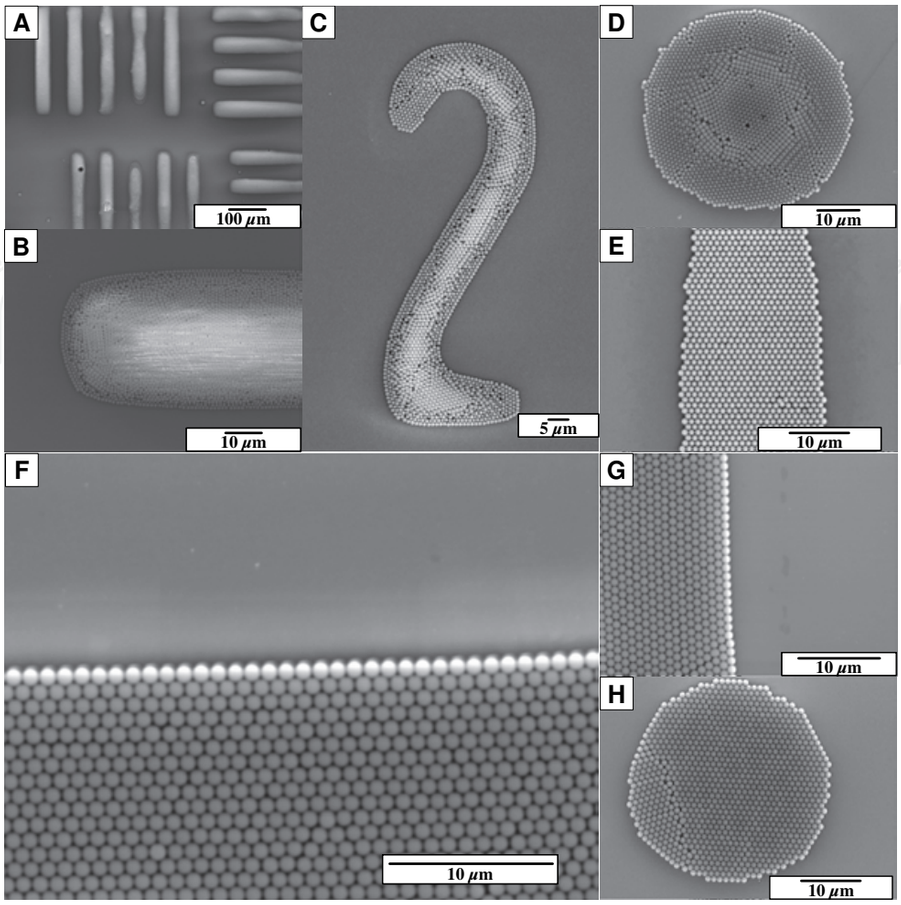

Reprinted with permission from Ref. [27], Masuda, Y., Itoh, T. and Koumoto, K., 2005, *Langmuir*, 21, 4478. Copyright @ American Chemical Society

Fig. 21. SEM micrographs of patterned colloidal photonic crystals constructed from (A-B) multi particle-layers, (C-D) partially double particle-layers or (E-H) single particle-layers. Image (B) is a magnified area of (A).

presented here are clearly higher than those previously reported[21-25]. Figure 4-2B shows a magnified area of the patterns constructed from thick particle-layers (Fig. 21A). The edge of patterns (Fig. 21, A to H) shows high feature edge acuity due to close-packing induced by meniscus force in the drying process. The core area of the particle circle (Fig. 21D, Fig. 22) was a double particle-layer of close-packed hexagonal lattice, i.e., the arrangement of fcc{111}, and the outer shell of the circle was a single particle-layer of hexagonal lattice (fcc{111}). The boundary area of these two flat terraces, i.e., inner shell, was constructed from a nested structure of square lattice, i.e., the arrangement of fcc{100}, to form a gentle slope between the core double-layer and outer shell single-layer. The lattice constant of the square lattice at the inner shell increased gradually with distance from the core of the circle to form a gentle slope. The difference in height was caused by the assembling process and the shape of the liquid mold in which the center is higher than the outside. The particle arrangement in the patterns constructed from a single particle-layer (Fig. 21, E to H) were assigned to the arrangement in fcc{111} which is a close-packed structure. The border line of particle layer in Fig. 21E showed different shape with that in Fig. 21F, G because the border

line of particle layer in Fig. 21F, G was fcc <1, 1, 0> and that in Fig. 21E was fcc <1/2, 1/2, 1> which is orthogonal to fcc <1, 1, 0>. There were far fewer defects in the particle patterns than in our former processes[21-25] because of the effective meniscus force. The standard deviation for the edge of the pattern constructed from a single particle-layer (Fig. 21F) was calculated in the same manner reported previously[24]. The center position ((x_i, y_i) μm) of each particle at the edge was plotted to estimate the standard deviation. The particle at the far left in the edge line of Fig. 21F was set to be the origin of the x-y coordinate.
The approximated straight line ($f(x)$) and its slope (θ) are represented as follows.

$$f(x) = 0.0273x - 0.09 \tag{7}$$

$$\cos\theta = 0.9996 \tag{8}$$

The standard deviation from the approximated straight line is given by the expression,

$$\text{S (standard deviation)} = \sqrt{U} = \frac{\left[\sum_i \left\{\cos\theta \cdot \left(f(x_i) - y_i\right)\right\}^2\right]^{1/2}}{n-1} \tag{9}$$

where n is the number of particles (n = 35). Unbiased variance (U) was used because the number of particles (n) is smaller than universe. The accuracy of the particle arrangement in Fig. 21F was estimated to be S = 8.75 × 10^{-3}. This is lower than that of the pattern constructed from a single particle-layer prepared in the solution using chemical reactions (S = 3.89 × 10^{-2}, Fig. 7 (a) in previous report[23]). The standard deviation for the edge of the pattern constructed from a single particle-layer (Fig. 21H) was calculated in the same manner.Distance (r_i) from center of a circle ((x_o, y_o) μm) to each particle ((x_i, y_i) μm) at the edge and its average ($\bar{r}$) are presented as follows.

$$r_i = \left((x_i - x_o)^2 + (y_i - y_o)^2\right)^{1/2} \tag{10}$$

$$\bar{r} = \frac{\sum_{i=1}^{n}\left((x_i - x_o)^2 + (y_i - y_o)^2\right)^{1/2}}{n} \tag{11}$$

x_o= 21.9 μm, y_o=17.7 μm, $\bar{r} = 16.53$ μm
The standard deviation from the approximated circle is given by the expression,

$$\text{S (standard deviation)} = \sqrt{V} = \left[\frac{\sum_{i=1}^{n}\left\{\left((x_i - x_o)^2 + (y_i - y_o)^2\right)^{1/2} - \bar{r}\right\}^2}{n}\right]^{1/2} \tag{12}$$

where n is the number of particles (n = 112). Variance (V) was used instead of unbiased variance because the number of particles (n) is the same as universe, i.e., all particles at the edge. The accuracy of the particle arrangement in Fig. 21H was estimated to be S = 3.89 × 10^1. This is higher than that in Fig. 21F because a perfect circle can't be constructed from a small number of particles which were packed in hexagonal arrangement.

The assembly process can be assumed from the details of structures and defects. Particle circles (Fig. 21, D and H) showed no defects at their core, implying that particles were probably assembled from the core of the particle circle and not from the outer shell. The particle circle (Fig. 21D, Fig. 22) would be formed not layer-by-layer, and the upper layer at

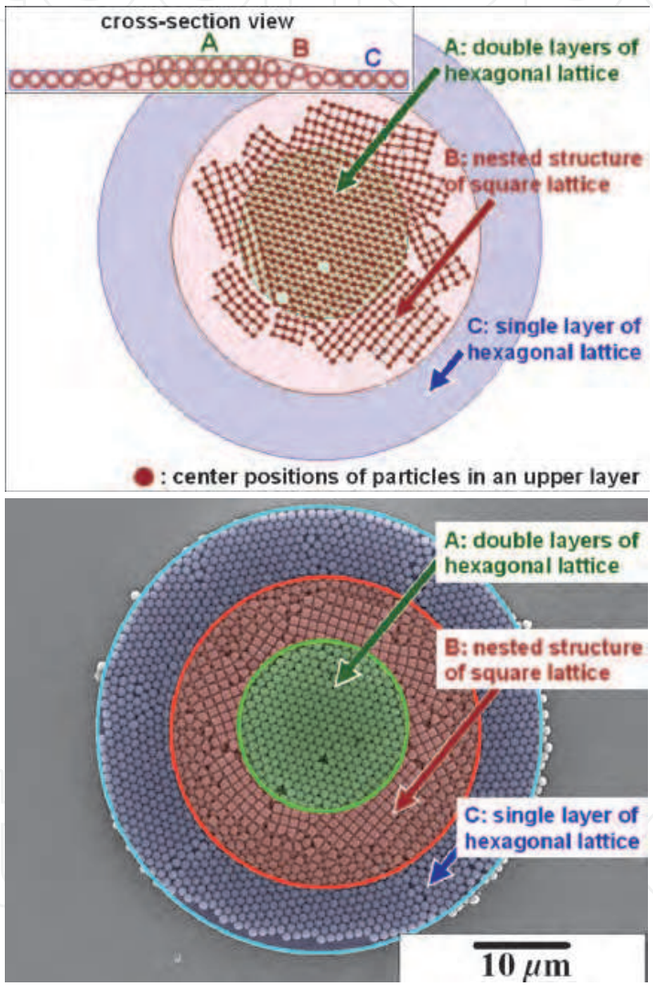

Reprinted with permission from Ref. [27], Masuda, Y., Itoh, T. and Koumoto, K., 2005, *Langmuir*, 21, 4478. Copyright @ American Chemical Society

Fig. 22. Particle arrangement view (top) prepared from SEM micrograph (bottom) of patterned colloidal photonic crystals constructed from partially double particle-layers. Center positions of particles in an upper layer show hexagonal or square lattice arrangement regions. The cross-sectional view shows the difference in height caused from the difference in particle arrangement modes. The three colored areas show regions of (A) double layers of hexagonal lattice, (B) nested structure of square lattice and (C) single layer of hexagonal lattice.

the core was also formed before the outer shell was assembled, since the first layer at the boundary area was not a close-packed assembly. A close-packed hexagonal lattice would be formed in the lower layer as shown in the single particle circle (Fig. 21H) in the case particles were assembled layer-by-layer. Other particle patterns (Fig. 21, A to C) would be assembled from the core area in the same manner.

Methanol solution containing particles was dropped onto a patterned OTS-SAM and dried in air without immersion into hexane for comparison. However, a particle pattern only with a low feature edge acuity was obtained. This indicates that the contact angle of methanol solution on OTS-SAM, i.e., the shape of the methanol solution mold, is important for particle patterning. Additionally, SiO_2 particles were dispersed in water instead of methanol, and a patterned OTS-SAM covered with the water colloidal solution was immersed into hexane, but the particle pattern was not obtained because the water solution cannot form a micropattern of the mold on hydrophilic regions selectively due to its high contact angle. These results suggest that the combination of methanol, hexane, OTS and silanol allowed us to fabricate micropatterns of particle assembly having high feature edge acuity and high regularity.

This two-solution self-assembly method successfully produced precise 2D patterns of colloidal photonic crystals, i.e., close-packed fcc or hcp particle assemblies having a photonic band gap, with short fabrication period and low energy. Various complicated patterns of colloidal crystals having high feature edge acuity and high regularity in particle assembly were fabricated, and the number of particle stacking layers, i.e., thickness of colloidal crystals, was demonstrated to be controlled. This process has the advantage of the drying process in which meniscus force can be utilized for close-packed particle assembly, and also the advantage of the static solution process in which particle assembling processes can be controlled well. The low dissolution rate of methanol into hexane and the appropriate contact angle of methanol on a substrate achieved by the combination of methanol, hexane, OTS and silanol allowed us to utilize the solution mold for particle patterning. Additionally, high dispersibility of particles and high repulsion force between particles and substrate suppressed the aggregation of particles, and the meniscus force between particles was effectively utilized to form a close-packed structure. The quality of SAM, shape and shrinkage rate of solution molds also greatly influence the feature edge acuity and the regularity of the particle assembly. The newly developed method achieved much higher regularity in particle assembly and feature edge acuity of the pattern than those previously reported[21-25]. The result is a step toward the realization of nano/micro periodic structures for next-generation photonic devices by the self-assembly process.

3.2 Self-assembly patterning of spherical colloidal crystals by two-solution method[28]

Micropatterns of spherical particle assemblies were fabricated by two-solution method[28]. Hydrophilic regions of a patterned self-assembled monolayer were covered with methanol solution containing SiO_2 particles and immersed in decalin to control the shape of droplets and gradually dissolve the methanol into decalin. Interfacing of methanol/decalin and shrinkage of methanol droplets were utilized to obtain meniscus force to form spherical particle assemblies; additionally, its static solution system allowed precise control of the conditions. Particles were assembled to form spherical shapes on hydrophilic regions of an SAM and consequently, micropatterns of spherical particle assemblies were successfully fabricated through self-assembly. This patterned two-solution process has the advantages of

both a drying process having meniscus force and a static solution process having high controllability.

An Si wafer (p-type Si [100], NK Platz Co., Ltd.) was sonicated in water, ethanol or acetone for 10 min, respectively, and exposed for 2 h to UV light (184.9 nm) (low-pressure mercury lamp, NL-UV253, Nippon Laser & Electronics Lab.) to clean the surface. The OTS-SAM or HFDTS-SAM[29] were prepared by immersing the Si substrate in an anhydrous toluene(Aldrich Chemical Co., Inc.) solution containing 1 vol% OTS(Acros Organics) or HFDTS(Lancaster synthesis Ltd.) for 5 min under an N_2 atmosphere (Fig. 23). The substrate with the SAM was baked at 120°C for 5 min to remove residual solvent and promote chemisorption of the SAM.

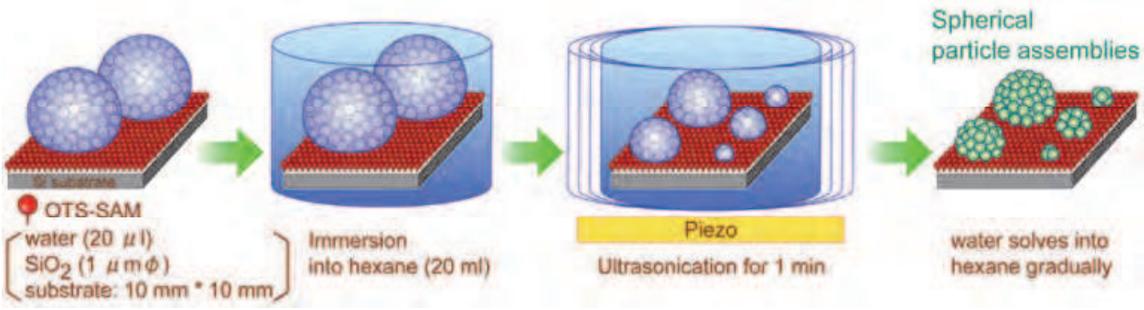

Reprinted with permission from Ref. [28], Masuda, Y., Itoh, T. and Koumoto, K., 2005, *Adv. Mater.*, 17, 841. Copyright @ Wiley-VCH Verlag GmbH & Co.

Fig. 23. Conceptual process for fabrication of spherical particle assemblies.

The HFDTS-SAM on the silicon substrate was exposed for 2 h to UV light through a photomask such as a mesh for transmission electron microscopy (Okenshoji Co., Ltd.) to be used as a template for micropatterning of spherical particle assemblies. UV-irradiated regions became hydrophilic due to silanol group formation, while the non-irradiated part remained unchanged. Formation of the SAMs and the modification to silanol groups by UV irradiation were verified using the water drop contact angle (θw). The initially deposited OTS-SAM or HFDTS-SAM showed a water contact angle of 105° or 112°, but the UV-irradiated surface of SAM was wetted completely (contact angle < 5°).

SiO_2 particles (1.13 μmφ, Hipresica UF N3N, CV: 3.57 %, specific gravity: 1.8 ± 0.1 g/cm^3, Ube-Nitto Kasei Co., Ltd.) (0.2 mg, 1.5 × 10^{27} particles) were thoroughly dispersed in water (20 μl) and dropped on a hydrophobic OTS(octadecyltrichlorosilane)-SAM (Fig. 23). The OTS-SAM with droplets was then immersed in hexane (20 ml, solubility of hexane in water at 20°C: 0.0013 g / 100 ml, specific gravity: 0.7) and ultrasonicated for 1 min. Large water droplets containing SiO_2 particles were separated into many small emulsions that kept them spherical on hydrophobic OTS-SAM. Water in the emulsions was gradually extracted to hexane to reduce the size of emulsions forming spherical particle assemblies[30]. After having been immersed for 12 h, spherical particle assemblies with different diameters were observed on OTS-SAM; it was also observed that the assemblies were constructed from various numbers of particles such as 3, 5, 6, 8 or many particles (Fig. 24, 25, 26). Quantities of 3, 5, 6 or 8 particles were assembled into triangular, pyramidal, octahedral or decahedral particle clusters, respectively. The number of particles in spheres can be controlled by the change of emulsion size or particle concentration in water[30]. The spherical shape of particle

assemblies was caused by the high contact angle of water emulsion on hydrophobic OTS-SAM in hexane. Consequently, various sizes of spherical particle assemblies can be prepared using this emulsion process.

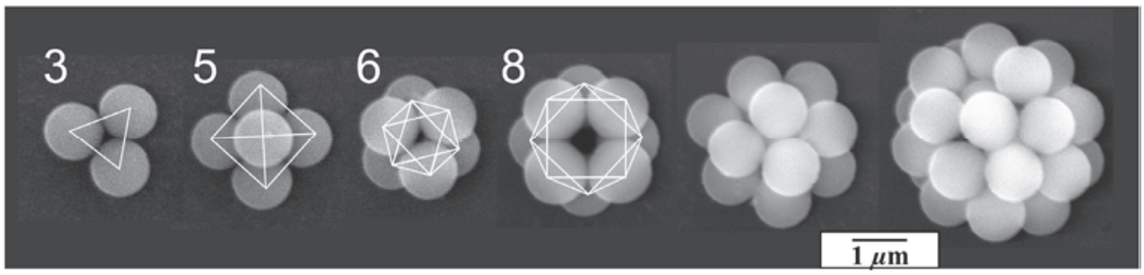

Reprinted with permission from Ref. [28], Masuda, Y., Itoh, T. and Koumoto, K., 2005, *Adv. Mater.*, 17, 841. Copyright @ Wiley-VCH Verlag GmbH & Co.

Fig. 24. SEM micrographs of spherical particle assemblies with different diameters. Particle assemblies constructed from a small number of particles such as 3, 5, 6, 8 and so on.

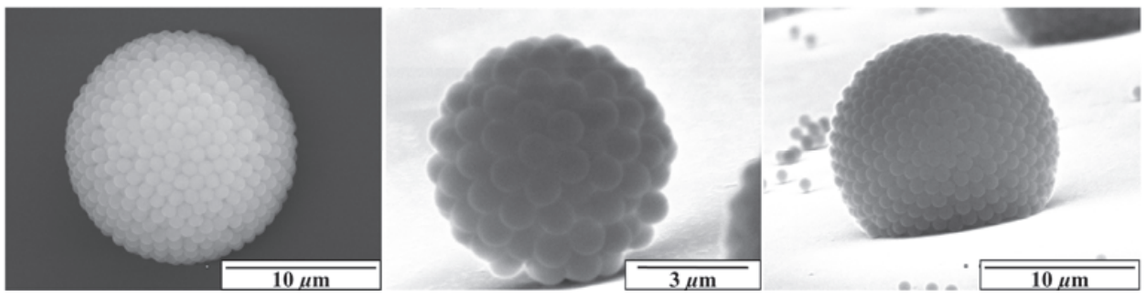

Reprinted with permission from Ref. [28], Masuda, Y., Itoh, T. and Koumoto, K., 2005, *Adv. Mater.*, 17, 841. Copyright @ Wiley-VCH Verlag GmbH & Co.

Fig. 25. Spherical particle assembly and tilted images.

The particles would be strongly bound to the droplet interfaces by surface tension in emulsions[31]. In the formation process of small clusters of particles (Fig. 24), the water in emulsions dissolved into hexane to reduce droplet size and this restricted the area in which particles could exist[30]. Particles touched together by the reduction of emulsion size and formed a spherically packed assembly. Deformation of the interface then led to the rearrangement that formed close-packed particle assemblies. The clusters were formed using emulsions not dispersed in the solution but adsorbed on the flat substrate, and thus some of the clusters showed imperfect symmetry such as pyramidal, octahedral or decahedral, which have a large flat face touching the substrate.

Additionally, large spherical particle assemblies (for instance ~57 μmφ in Fig. 26) were prepared from large methanol emulsions (~100–300 μmφ) in decalin (decahydronaphthalene) without the use of ultrasonication, which makes emulsions smaller. Many linear disclinations, i.e., grain boundaries, were formed on the surface to reduce elastic strain energy because a close-packed triangular particle lattice composed of a particle

surrounded by 6 particles in plane cannot cover a spherical surface[32]. Linear disclinations were composed of an alternative arrangement of the particle surrounded by 5 particles in plane (red, this particle can be assumed to have a charge of +1) and the particle surrounded by 7 particles in plane (yellow, charge –1). Both ends of a linear disclination were particles surrounded by 5 particles in plane to make the total charge of each linear disclination +1 as observed in previous report[32]. The minimum number of linear disclinations can be calculated for the large sphere (~57 μmφ) (Fig. 26) to be 22 (N: minimum number of linear disclinations $N = 12 + 0.41r/d = 22$, r: radius of sphere ~28.5 μm, d: mean particle spacing 1.13 μm) from geometric calculations[32,33]. The surface area in a purple circle can be also calculated to be about 10.5 % of the total surface area of the sphere from the formula (surface area ratio: S_2/S_1, surface area of the sphere: $S_1 = 4\pi r^2$, surface area in a purple circle: $S_2 = 2\pi r(r - r_1)$, radius of the purple circle shown in Fig. 26 $\sqrt{r^2 - r_1^2} = 17.5\mu$m). The minimum number of linear disclinations on the surface area in a circle can therefore be estimated to about 2.3(n: minimum number of linear disclinations in a purple circle $n = N \cdot S_2/S_1$). However, many linear disclinations were observed in an SEM micrograph (Fig. 26 (Right)). It is suggested that our assembly method can be further optimized to reduce linear disclinations.

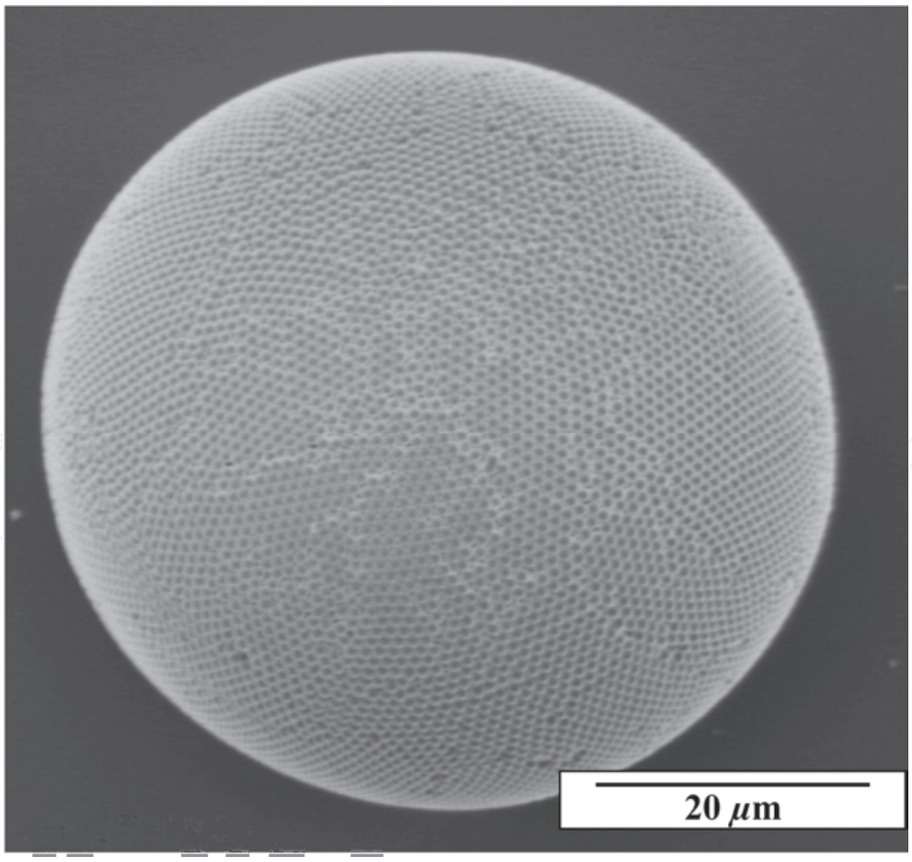

Fig. 26. (Continued)

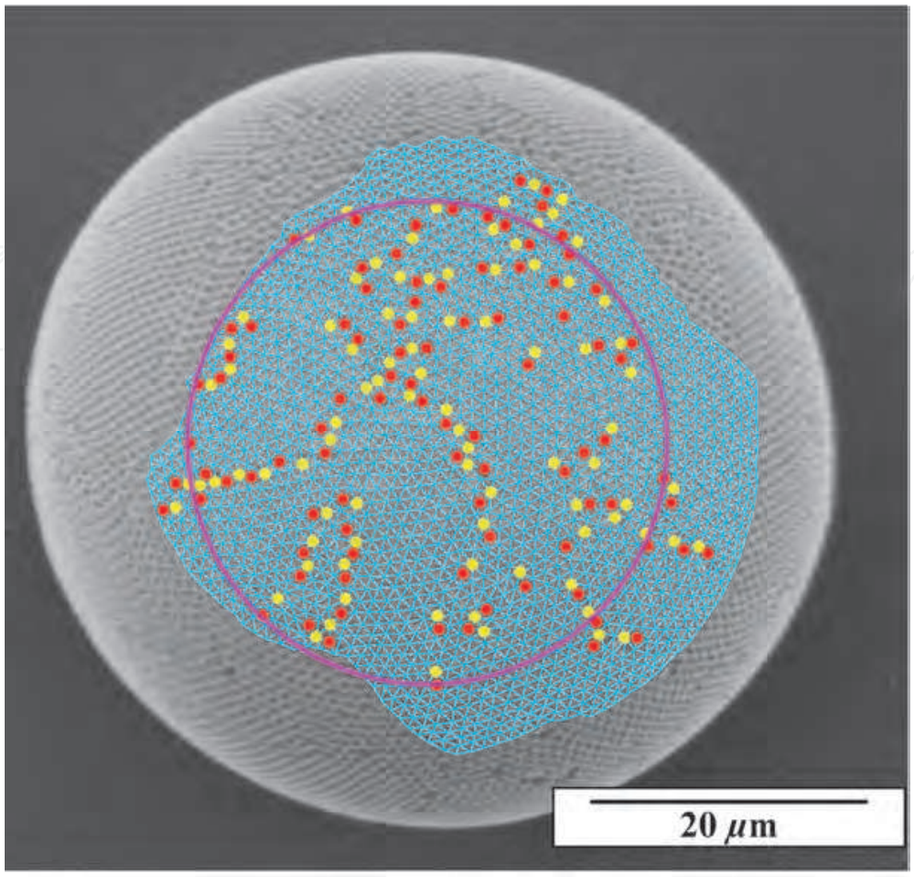

Reprinted with permission from Ref. [28], Masuda, Y., Itoh, T. and Koumoto, K., 2005, *Adv. Mater.*, 17, 841. Copyright @ Wiley-VCH Verlag GmbH & Co.

Fig. 26. Top: A large spherical particle assembly. Bottom: Linear disclinations on a large spherical particle assembly.

Furthermore, the upper sides of spherical particle assemblies were removed using a manipulator installed in an optical microscope (BX51WI Microscope, Olympus Optical Co., Ltd.) to evaluate the packing structure. Particle assemblies have a densely packed structure (Fig. 27). Particles would be completely rearranged to form a densely packed structure during the reduction of emulsion size due to the high dispersibility of particles in emulsions. SiO_2 particles (1.13 μmφ, 1 g/l) were thoroughly dispersed in methanol solution (10 μl) and dropped onto a patterned HFDTS(heptadecafluoro-1,1,2,2-tetrahydrodecyltrichlorosilane)-SAM[29] having hydrophobic HFDTS-SAM regions and hydrophilic silanol regions, photopatterned using a mesh for transmission electron microscopy as a photomask (Fig. 28). The patterned SAM covered with the solution was then carefully immersed in decalin so as not to remove the solution because the density of methanol (0.79) is lower than that of decalin (0.88) causing methanol to float on decalin. The patterned SAM was then gently vibrated to remove additional methanol solution and assist the movement of droplets to silanol regions. The methanol solution was selectively contacted on hydrophilic regions to form a micropattern of the solution, which became clearer after immersion for a few hours. The methanol solution containing particles formed a spherical shape because of the surface

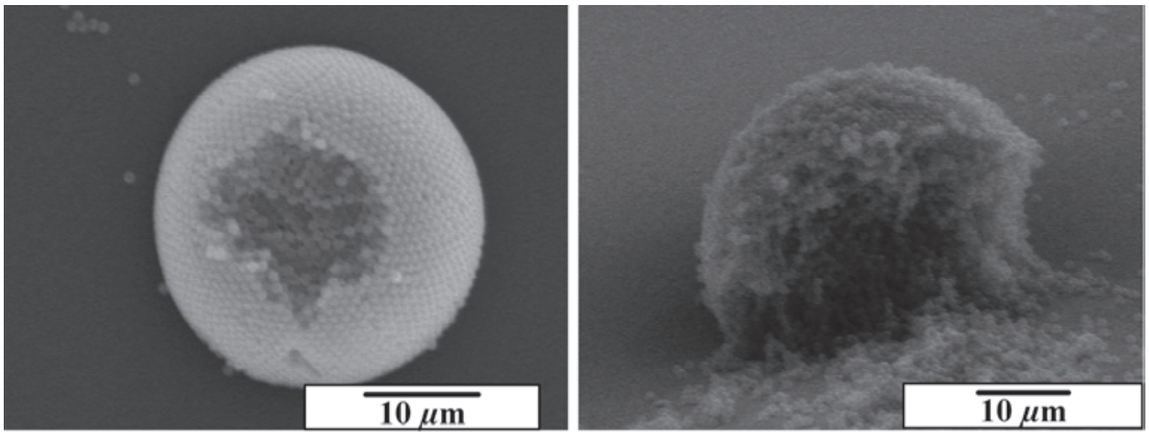

Reprinted with permission from Ref. [28], Masuda, Y., Itoh, T. and Koumoto, K., 2005, *Adv. Mater.*, 17, 841. Copyright @ Wiley-VCH Verlag GmbH & Co.

Fig. 27. SEM micrographs showing the inside of spherical particle assemblies formed from methanol emulsions in decalin.

interaction between methanol, decalin and surface of a SAM and the buoyant force of methanol in decalin. Methanol in emulsions was gradually dissolved into exterior decalin phase to form particle assemblies. After having been immersed for 12 h, particle assemblies having a dome shape were formed at the center of each silanol region (Fig. 29). The distance between the centers of each spherical particle assembly was same to the distance between holes of a mesh. The diameter of spherical particle assemblies was about 18 μmφ. It was smaller than that of hydrophilic regions (about 100μm) due to low particle concentration in methanol and the shape of methanol droplets on a substrate. This indicates the arrangement regularity of spherical particle assemblies can be improved more by the use of the photomask having small holes to decide positions of each droplet precisely. Some extra particles, i.e., noise particles, were also deposited on hydrophobic regions. The process should be further optimized to control many factors such as volume of methanol solution on a substrate, quality of a SAM or aggregation of particles in the solution to avoid noise particles. Particle assemblies were shown to have a densely packed structure by destructive inspection using a manipulator. Consequently, the dot array of spherical particle assemblies was successfully fabricated by this self-assembly process.

Micropatterns of particle assemblies were fabricated without the use of a template, having microstructures such as molds or grooves. A two-dimensional array of spherical particle assemblies was fabricated by self-assembly with this method. Interfacing between two solutions and shrinkage of droplets were utilized to obtain meniscus force to form spherical particle assemblies, and additionally, its static solution system allowed precise control of the conditions. These showed the high ability of self-assembly processes to prepare microstructures constructed from colloidal crystals. Further investigations of the solution-solution, solution-SAMs and solution-particles interfaces and the behavior of particles and solutions would allow us to develop this two-solution system to prepare desirable particle assembly structures.

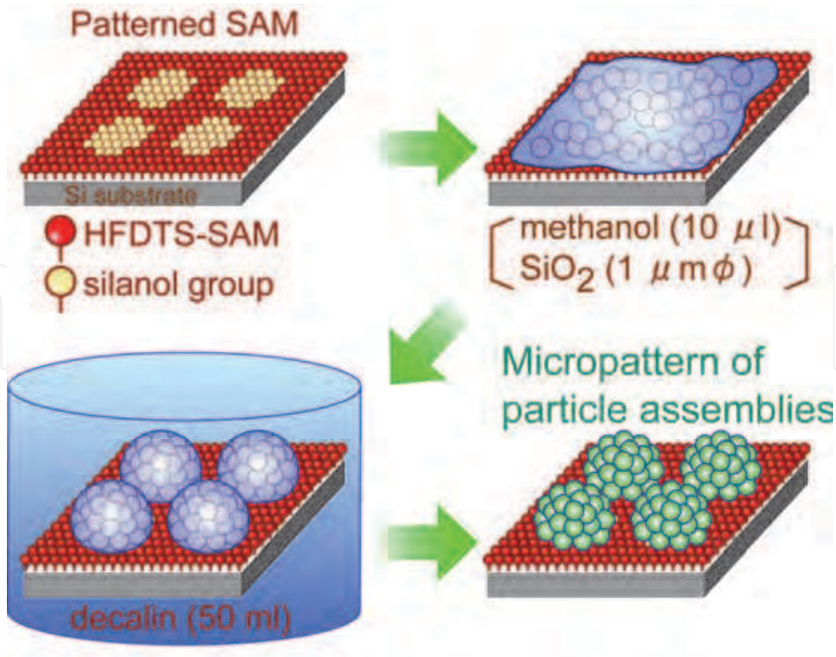

Reprinted with permission from Ref. [28], Masuda, Y., Itoh, T. and Koumoto, K., 2005, *Adv. Mater.*, 17, 841. Copyright @ Wiley-VCH Verlag GmbH & Co.

Fig. 28. Conceptual process of micropattern of spherical particle assemblies.

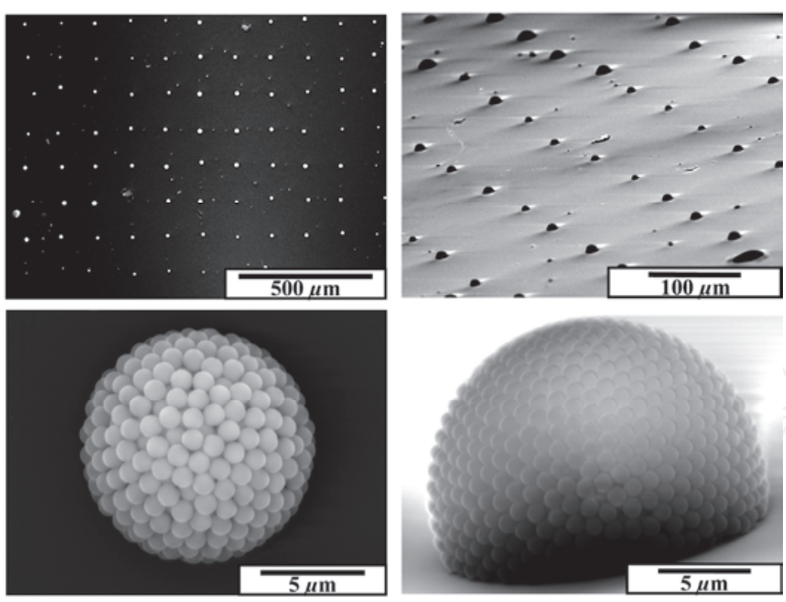

Reprinted with permission from Ref. [28], Masuda, Y., Itoh, T. and Koumoto, K., 2005, *Adv. Mater.*, 17, 841. Copyright @ Wiley-VCH Verlag GmbH & Co.

Fig. 29. SEM micrographs of micropattern of spherical particle assemblies. Top left: Micropattern of spherical particle assemblies. Bottom left: Magnified area of top left. Top right: Tilted micropattern of spherical particle assemblies. Bottom right: Magnified area of top right.

4. Summary

Self-assembly patterning of colloidal crystals was realized by liquid phase patternig, drying patterning and two-solution method. Micropatterns of colloidal crystals were fabricated under environmentally friendly conditions using self-assembled monolayers. They can be applied to photonic crystals, dye-sensitized solar cell, molecular sensors, gas sensors, nano-particle devices, etc. These showed high ability of self-assembled monolayers and self-assembly processes.

5. References

[1] Masuda, Y.; Koumoto, K. *J. Soc. Inor. Mater. Jpn.* 2000, *7*, 4-12.
[2] Masuda, Y.; Tachibana, K.; Itoh, M.; Koumoto, K. *Materials Integration* 2001, *14*, 37-44.
[3] Yablonovitch, E. *Phys. Rev. Lett.* 1987, *58*, 2059-2062.
[4] John, S. *Phys. Rev. Lett.* 1987, *58*, 2486-2489.
[5] Joannopoulos, J. D.; Meade, R. D.; Winn, J. N. *Princeton Press, Princeton, New Jersey* 1995.
[6] Chow, E.; Lin, S. Y.; Johnson, S. G.; Villeneuve, P. R.; Joannopoulos, J. D.; Wendt, J. R.; Vawter, G. A.; Zubrzycki, W.; Hou, H.; Alleman, A. *Nature* 2000, *407*, 983-986.
[7] Colombelli, R.; Srinivasan, K.; Troccoli, M.; Painter, O.; F. Gmachl, C.; Tennant, D. M.; Sergent, A. M.; Sivco, D. L.; Cho, A. Y.; Capasso, F. *Science* 2003, *302*, 1374-1377.
[8] Noda, S.; Tomoda, K.; Yamamoto, N.; Chutinan, A. *Science* 2000, *289*, 604-606.
[9] M. Qi; E. Lidorikis; P. T. Rakich; S. G. Johnson; J. D. Joannopoulos; E. P. Ippen; H. I. Smith *Nature* 2004, *429*, 538-542.
[10] M. Campbell; D. N. Sharp; M. T. Harrison; R. G. Denning; A. J. TurberReld *Nature* 2000, *404*.
[11] J. G. Fleming; S. Y. Lin *Optics Letters* 1999, *24*, 49-51.
[12] S. R. Kennedy; M. J. Brett; O. Toader; S. John *Nano Letters* 2002, *2*, 59-62.
[13] Kuramochi, E.; Notomi, M.; Kawashima, T.; Takahashi, J.; Takahashi, C.; Tamamura, T.; Kawakami, S. *Optical and Quantum Electronics* 2002, *34*, 53-61.
[14] Vlasov, Y. A.; Bo, X. Z.; Sturm, J. C.; Norris, D. J. *Nature* 2001, *414*, 289-293.
[15] A. Blanco; E. Chomski; S. Grabtchak; M. Ibisate; S. John; S. W. Leonard; C. Lopez; F. Meseguer; H. Miguez; J. P. Mondia; G. A. Ozin; O. Toade; H. M. van Driel *Nature* 2000, *405*, 437-440.
[16] Xia, N.; Gates, B.; Yin, Y.; Lu, Y. *Adv. Mater.* 2000, *12*, 693-713.
[17] Lopez, C. *Adv. Mater.* 2003, *15*, 1679-1704.
[18] Kim, E.; Xia, Y.; Whitesides, G. M. *Adv. Mater.* 1996, *8*, 245-247.
[19] Ozin, G. A.; Yang, S. M. *Adv. Func. Mater.* 2001, *11*, 95-104.
[20] Xia, Y. N.; Yin, Y. D.; Lu, Y.; McLellan, J. *Adv. Func. Mater.* 2003, *13*, 907-918.
[21] Masuda, Y.; Seo, W. S.; Koumoto, K. *Thin Solid Films* 2001, *382*, 183-189.
[22] Masuda, Y.; Seo, W. S.; Koumoto, K. *Jpn. J. Appl. Phys.* 2000, *39*, 4596-4600.
[23] Masuda, Y.; Itoh, M.; Yonezawa, T.; Koumoto, K. *Langmuir* 2002, *18*, 4155-4159.
[24] Masuda, Y.; Tomimoto, K.; Koumoto, K. *Langmuir* 2003, *19*, 5179-5183.
[25] Masuda, Y.; Itoh, M.; Koumoto, K. *Chem. Lett.* 2003, *32*, 1016-1017.
[26] Masuda, Y.; Itoh, T.; Itoh, M.; Koumoto, K. *Langmuir* 2004, *20*, 5588-5592.
[27] Masuda, Y.; Itoh, T.; Koumoto, K. *Langmuir* 2005, *21*, 4478-4481.
[28] Masuda, Y.; Itoh, T.; Koumoto, K. *Adv. Mater.* 2005, *17*, 841-845.
[29] Masuda, Y.; Sugiyama, T.; Koumoto, K. *J. Mater. Chem.* 2002, *12*, 2643-2647.

[30] Manoharan, V. N.; Elsesser, M. T.; Pine, D. J. *Science* 2003, *301*, 483-487.
[31] Levine, S.; Bowen, B. D.; Partridge, S. J. *Colloids and Surfaces* 1989, *38*, 325-343.
[32] Bausch, A. R.; Bowick, M. J.; Cacciouto, A.; Dinsmore, A. D.; Hsu, M. F.; Nelson, D. R.; Nikolaides, M. G.; Travesset, A.; Weitz, D. A. *Science* 2003, *299*, 1716-1718.
[33] Bowick, M. J.; Nelson, D. R.; Travesset, A. *Phys. Rev. B* 2000, *62*, 8738-8751.

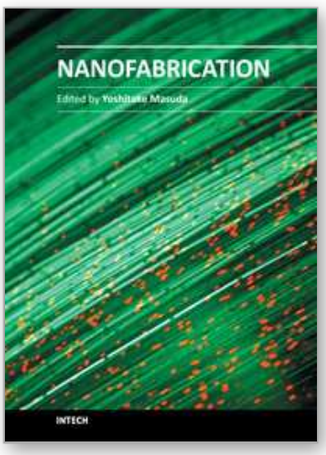

Nanofabrication

Edited by Dr. Yoshitake Masuda

ISBN 978-953-307-912-7
Hard cover, 354 pages
Publisher InTech
Published online 22, December, 2011
Published in print edition December, 2011

We face many challenges in the 21st century, such as sustainably meeting the world's growing demand for energy and consumer goods. I believe that new developments in science and technology will help solve many of these problems. Nanofabrication is one of the keys to the development of novel materials, devices and systems. Precise control of nanomaterials, nanostructures, nanodevices and their performances is essential for future innovations in technology. The book "Nanofabrication" provides the latest research developments in nanofabrication of organic and inorganic materials, biomaterials and hybrid materials. I hope that "Nanofabrication" will contribute to creating a brighter future for the next generation.

How to reference

In order to correctly reference this scholarly work, feel free to copy and paste the following:

Yoshitake Masuda (2011). Nanofabrication of Particle Assemblies and Colloidal Crystal Patterns, Nanofabrication, Dr. Yoshitake Masuda (Ed.), ISBN: 978-953-307-912-7, InTech, Available from: http://www.intechopen.com/books/nanofabrication/nanofabrication-of-particle-assemblies-and-colloidal-crystal-patterns

INTECH
open science | open minds

InTech Europe
University Campus STeP Ri
Slavka Krautzeka 83/A
51000 Rijeka, Croatia
Phone: +385 (51) 770 447
Fax: +385 (51) 686 166
www.intechopen.com

InTech China
Unit 405, Office Block, Hotel Equatorial Shanghai
No.65, Yan An Road (West), Shanghai, 200040, China
中国上海市延安西路65号上海国际贵都大饭店办公楼405单元
Phone: +86-21-62489820
Fax: +86-21-62489821

IntechOpen